

Patterns on growing square domains via mode interactions

Adela Comanici^a and Martin Golubitsky^{b*}

^a*Department of Mathematics, Virginia Tech, Blacksburg, VA 24061-0123;* ^b*Department of Mathematics, University of Houston, Houston, TX, 77204-3008*

(Received 8 May 2007; final version received 7 December 2007)

Numerical simulations of reaction-diffusion systems with Neumann boundary conditions (NBC) on growing square domains by Maini et al. exhibit square and stripe (or roll) patterns that are usually associated with bifurcations from a trivial equilibrium on a square lattice. However, these patterns change as the domain grows. In this article we discuss several of these transitions; namely, transitions between different types of squares and between squares and stripes (or rolls). We show that these transitions can be understood by tracing paths through the unfoldings of certain co-dimension two mode interactions. To understand these transitions, we need to discuss two issues: the speed at which the domain size changes and the relations between NBC and periodic boundary conditions (PBC) on a square. First, in the simulations, the domain growth takes place on a time scale that is longer than the one needed for pattern formation. Therefore, we can assume that the domain growth is identified with quasistatic variation of time; that is, the domain grows slowly enough that the PDE solution of the time-dependent system tracks equilibria of the reaction-diffusion systems posed on a fixed size domain. Second, as is well-known, NBC problems on a square of side length l can be embedded in PBC problems on a square with side length $2l$. The PBC problem has translation symmetries that are not present in the NBC problem. These additional symmetries are called *hidden symmetries* in the literature. Moreover, solutions to PBC that restrict to the smaller square and satisfy NBC are just those solutions that satisfy certain symmetry constraints. We show further that the transitions between different patterns can be understood by considering relevant mode interaction bifurcation problems on the larger square and then restricting to the smaller square. We have found that a generic continuous transition can occur between two types of squares. Also, the transition between squares and stripes can generically occur either via steady states and time-periodic states (*standing waves*) or via a jump. Interestingly, in mode interactions, the symmetry constraints induced by NBC are important in understanding which solutions exist and which solutions are stable. For example, diagonal stripes cannot occur as a primary branch in the NBC problem but do in the PBC problem. Also, patterns can be stable in the NBC problem that are not stable in the PBC problem. As a consequence, in the NBC problem we see *standing wave* time-periodic solutions as stable patterns leading to stable stripes, whereas in the PBC problem we see *wavy rolls* steady states as stable patterns leading to stable stripes. In principle, a classification of all transitions in NBC mode interactions is possible. However, we concentrate only on those transitions that are relevant to the numerically observed transitions.

*Corresponding author. Email: mg@uh.edu

Keywords: Pattern Formation; Growing Domains; Mode Interaction; Bifurcation; Symmetry

1. Introduction

Turing [1] proposed that reaction-diffusion models can be used to explain pattern formation in various biological systems. He demonstrated theoretically that a system of two reacting and diffusing chemical concentrations, termed *morphogens*, could give rise to spatial patterns in these concentrations via a chemical instability process now called a *Turing instability* or a *diffusion-driven instability*. Turing patterns were first found by Castets et al. [2] in a chloride-ionic-malonic-acid (CIMA) reaction. Ouyang and Swinney [3] were the first to observe Turing instability from a spatially uniform state to a patterned state. Morphogens have been identified in some biological systems [4], but nevertheless the issue of self-organization via the Turing instability is highly controversial [5]. The Turing theory for pattern formation on fixed domains has been criticized in part because it is difficult to identify the morphogens that are responsible for the patterns.

1.1. Growing domains

Growing domains have the mathematical effect of decreasing diffusion rates and hence increasing the likelihood of crossing a Turing instability [6]. More precisely, [7,8] note that a reaction-diffusion system on a growing domain with Neumann boundary conditions (NBC) can be transformed into a reaction-diffusion system with NBC on a fixed domain, but with time-dependent diffusion terms and time-dependent dilution terms. Since growing domains effectively change diffusion rates, the identification of the exact morphogens is less crucial in determining instabilities. Thus, the mathematical understanding of the effects of domain growth on Turing patterns is an important problem.

Kondo and Asai [9] illustrate the role of domain growth in pattern formation in biological species by finding mode doubling in the patterns of the angelfish *Pomacanthus* as it grows. The juvenile *Pomacanthus*, which is less than 2 cm long, has three dorsoventral or vertical stripes; once the fish grows to twice this length, new stripes emerge between the original stripes so that the original wavelength is maintained.

Numerical simulations on one-dimensional growing domains with different growth functions are shown in [6,7,10]. Similarly, numerical simulations of reaction-diffusion systems with NBC on two-dimensional growing domains (square, conical, circular, hexagonal, triangular and rectangular domains) are shown in [7,8,11,12]. All of these simulations use reaction-diffusion systems with NBC on fixed square domains and with time-dependant diffusion and dilution terms (see [8]).

We focus on two transitions between patterns in the numerical simulations of a reaction-diffusion system on a growing square domain: one observed in Plaza et al. [8] and one in Madzvamuse et al. [1]. In this article we show how these two observed transitions can be understood in the context of equivariant bifurcation theory, specifically as paths through a certain co-dimension two mode interaction. In this introduction, we present the relevant numerical results, recall how modes arise from NBC and hidden symmetries, and specify the mode interaction that is to be studied.

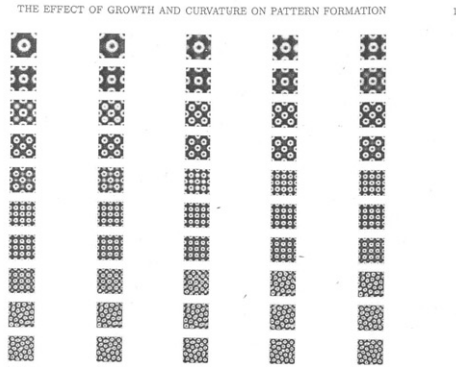


Figure 1. Transitions between different types of square patterns on a unit square domain with NBC and growth function $\rho(t) = 1 + 0.0005t$.
Notes:

$$u_t = 0.899u(1 - 0.5v^2) + v(1 - 0.4u) + \frac{0.516}{\rho^2} \Delta u - \frac{10^{-3}}{\rho} u$$

$$v_t = u(-0.899 + 0.4u) + v(-0.91 + 0.4995u) + \frac{1}{\rho^2} \Delta u - \frac{10^{-3}}{\rho} v.$$

Results from [8]; the sequence of pictures should be read by rows, starting at the top.

1.2. Numerical simulations on square domains

The numerical simulations by Plaza et al. [8] of a reaction-diffusion system on a square domain growing isotropically and linearly in time with a growth function $\rho(t)$ are reproduced in Figure 1. (Similar results are obtained by Crampin [7] using Schnakenberg kinetics.) We concentrate on the first four pictures in row 1 in this figure. Each of these pictures has square symmetry, but there is a difference in the pattern between the first three and the fourth. We show below that the first three correspond to a (2, 0)-mode and the fourth to a (2, 2)-mode. See Figure 2.

The numerical simulations of Madzvamuse et al. [11] use a reaction-diffusion system with Schnakenberg kinetics on a square domain growing exponentially in time and some of their results are reproduced in Figure 3. Observe that the first picture corresponds to squares (the (2, 2)-mode mentioned above) and the second to stripes. We show below that the stripes in this figure correspond to a (2, 0)-mode. There is no indication in Figure 3 of how the transition from squares to stripes actually occurs.

Both of these numerical simulations suggest that the theoretical study of steady state (2, 0) and (2, 2)-mode interactions may be helpful in understanding the observed transitions. We will show that both of these transitions of pattern can be found in paths through the unfolding of such co-dimension two bifurcations. To explain our results we need to discuss the relationship between a growing domain problem and a bifurcation problem, the existence of hidden symmetries for reaction-diffusion systems on square domains with NBC and the way that these hidden symmetries relate to modes.

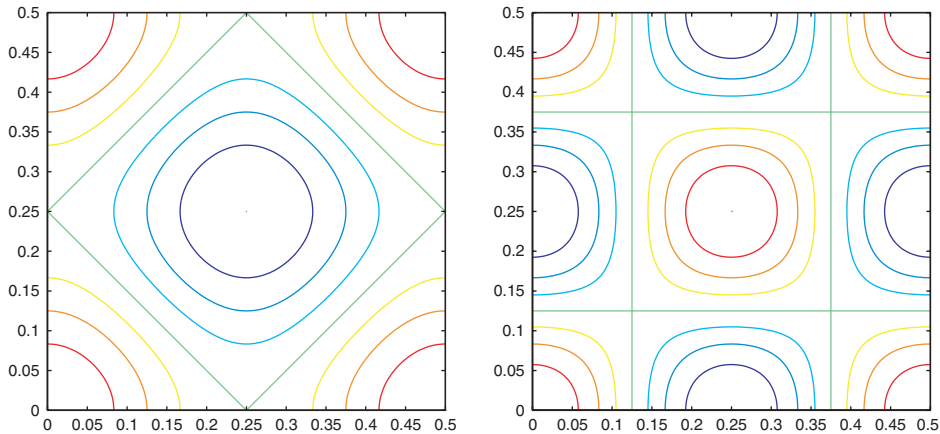


Figure 2. Square planforms restricted to $[0, (1/2)] \times [0, (1/2)]$.
 Notes: (Left) mode (2,0); level curves of $e^{4\pi i x} + e^{4\pi i y} + \text{c.c.}$ (Right) mode (2,2); level curves of $e^{4\pi i(x+y)} + e^{4\pi i(x-y)} + \text{c.c.}$

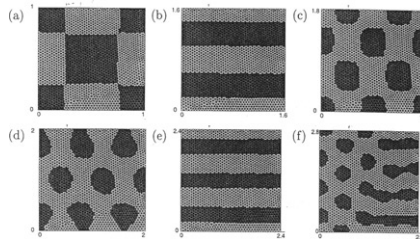


Figure 3. Transitions between squares and stripes on a unit square domain with NBC and growth function $\rho(t) = e^{\sigma t}$ with $10^{-5} \leq \sigma \leq 10^{-2}$.
 Notes:

$$\begin{aligned}
 u_t &= 230.82(0.1 - u + u^2 v) + \frac{1}{\rho} \Delta u - \sigma u \\
 v_t &= 230.82(0.9 - u^2 v) + \frac{8.6676}{\rho^2} \Delta v - \sigma
 \end{aligned}$$

Results from [11]; the sequence of pictures should be read by rows, starting at the top.

1.3. Pattern transitions in growing domains and bifurcations

Our approach to pattern transition is based on quasistatic variation of time through frozen systems. More precisely, for each time t_0 we freeze the time-dependent diffusion rates and dilution terms in the reaction-diffusion system on the fixed square domain, and then we attempt to determine the asymptotically stable states of the *frozen* system. We assume that the domain growth is on a time scale that is much longer than the time scale than it takes the system to approach an asymptotic state in the frozen system. In this way, time becomes a bifurcation parameter which, manifests itself through the quasistatic variation of diffusion rates. Although we do not prove that this method is rigorous, we note that a similar bifurcation theoretic approach is used by Izhekevich [13] to describe different kinds of bursting in two time-scale systems.

In this scenario, pattern transitions correspond to bifurcations between asymptotic states as the diffusion rates vary. Specifically we study co-dimension two bifurcations where steady states corresponding to the desired patterns (squares, stripes, etc.) coalesce. We identify the variation of t_0 with a path through the two-dimensional unfolding space of a co-dimension two bifurcation (a parameter plane). We determine, as is typically done in multiparameter bifurcation theory, the regions in the parameter plane where equilibria and periodic orbits exist and are stable. In the bifurcation problems we study, each equilibrium corresponds to a different patterned state. Thus, pattern transitions are identified with paths in parameter plane that cross boundaries where changes in the existence of stable states occur. This approach was used in [14], where numerical simulation of paths through unfoldings did successfully describe different kinds of bursting phenomena.

Stated in another way, by tracing a path in the parameter plane, we create a bifurcation diagram that shows the equilibria and the periodic orbits of these systems as time t_0 varies. Our assumption on time scales implies that the solution to the time-dependent PDE system will track the asymptotically stable solutions on this bifurcation diagram. In this sense, the growing domain can be considered as quasistatic variation of time through a bifurcation diagram.

In this article we construct the possible bifurcation diagrams from mode interaction bifurcations in the frozen systems. Hidden symmetry is an important component of this analysis. We have found that the study of a relevant mode interaction gives a theoretical basis for the results of the numerical simulations. Indeed, there are paths that lead to continuous transition between the two types of squares patterns, and there are paths that lead to a transition between squares and stripes (via either intermediate steady states and time-periodic states, or via a jump).

1.4. Hidden symmetries

Crawford et al. [15] observe that a reaction-diffusion system with NBC on a square domain can be viewed as the restriction of the same reaction-diffusion system with periodic boundary conditions (PBC) on a double side-length square domain and that this extension has much greater symmetry than did the original NBC problem. These extra symmetries are called *hidden symmetries*. This extension is accomplished by reflecting twice across the horizontal and vertical boundaries of the small square.

Specifically, suppose that the small square is given by $0 \leq x, y \leq \ell$ and that a solution $u(x, y)$ to a reaction-diffusion system on that square satisfies NBC, that is,

$$u_y(x, 0) = 0 = u_y(x, \ell) \quad \text{and} \quad u_x(0, y) = 0 = u_x(\ell, y) \tag{1.1}$$

Then extend u to the square $0 \leq x, y \leq 2\ell$ by setting

$$u(2\ell - x, y) = u(x, 2\ell - y) = u(2\ell - x, 2\ell - y) = u(x, y) \tag{1.2}$$

It is well-known that the extended u is a solution to the same reaction-diffusion system and that u satisfies PBC, that is,

$$\begin{aligned} u(0, y) &= u(2\ell, y) & u_{xx}(0, y) &= u_{xx}(2\ell, y) \\ u(x, 0) &= u(x, 2\ell) & u_{yy}(x, 0) &= u_{yy}(x, 2\ell) \end{aligned} \tag{1.3}$$

Moreover, any solution to the reaction-diffusion system on the larger square with PBC (1.3), that also satisfies the symmetry constraint (1.2), automatically satisfies NBC (1.1) on the small square.

This extension has the following consequence. The domain symmetry group of the reaction-diffusion system on the small square satisfying NBC is the group \mathbf{D}_4 , the eight-element dihedral group of symmetries of the square generated by the rotation and reflection

$$(x, y) \mapsto (y, x) \quad \text{and} \quad (x, y) \mapsto (\ell - x, y)$$

whereas the domain symmetry group of the system on the large square satisfying PBC is the group $\mathbf{D}_4 \times \mathbf{T}^2$, where \mathbf{D}_4 is generated by the rotation ξ and the reflection η defined by

$$\xi(x, y) = (-y, x) \quad \text{and} \quad \eta(x, y) = (2\ell - x, y) \quad (1.4)$$

The torus group \mathbf{T}^2 consists of translations in \mathbf{R}^2 modulo the spatial period 2ℓ , that is,

$$(x, y) \mapsto (x + x_0, y + y_0)$$

for any $(x_0, y_0) \in \mathbf{R}^2$.

These additional symmetries change the generic behaviour of the NBC problem in two ways. First, the torus symmetry allows us to equate generic co-dimension one bifurcations with modes. Second, as discussed in Crawford [16], the details of co-dimension two steady state mode interactions in the NBC case are quite different from those mode interactions that involve only \mathbf{D}_4 symmetry. There is a long history of studies of the effect of hidden symmetries, see [15,17]. In particular, the work of Crawford et al. [16,18] demonstrates that hidden symmetries can lead to predictable, physically observable effects in the Faraday experiment.

There is a notational inconvenience that we must discuss here. The simulations using NBC described below were computed on the unit square ($\ell = 1$). The PBC theory that we will discuss is most easily developed on that same unit square, but now with PBC ($\ell = 1/2$).

1.5. Modes in $\mathbf{D}_4 \times \mathbf{T}^2$ -bifurcation problems

As is well-known [17,19] the study of bifurcations in a reaction-diffusion system on a square with PBC is equivalent to the study of bifurcations in that same reaction-diffusion system on the plane restricted to the space of planar spatially doubly periodic functions. More precisely, let \mathcal{L} be the square lattice generated by the vectors $(1, 0)$, $(0, 1)$. We can rewrite a reaction-diffusion system on the square as an operator on functions that are doubly periodic with respect to the square lattice.

Let L_0 be the linearization at a *trivial* spatially homogeneous steady state. Let $k = (k_1, k_2) \in \mathbf{Z}^2$ be a *dual wave vector*; that is, the associated *plane wave* $e^{2\pi i k \cdot (x, y)}$ is an \mathcal{L} doubly periodic function. Due to \mathbf{T}^2 symmetry, all eigenfunctions of L_0 have plane wave factors. It is again well-known that generically $\ker L_0$ consists of all critical eigenfunctions with a given *critical wave number* k_c . That is

$$\ker L_0 \cong \sum_{|k|=k_c} z_k e^{2\pi i k \cdot (x, y)} + \text{c.c.} \quad (1.5)$$

where $z_k \in \mathbf{C}$ and c.c. indicates the complex conjugate.

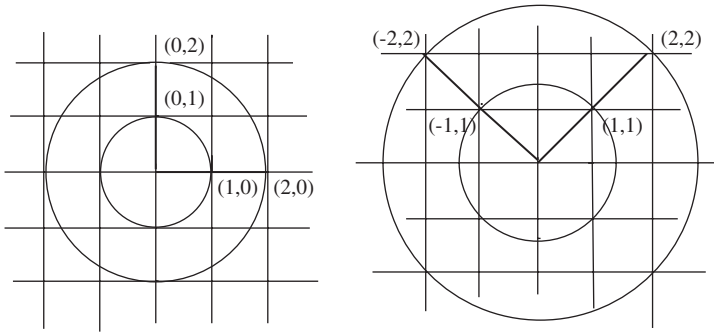


Figure 4. $(1, 0), (2, 0)$ -modes (left) and $(1, 1), (2, 2)$ -modes(right) in PBC.

Typically, a symmetry-breaking bifurcations lead to kernels of L_0 whose dimension is either four or eight. When $k_c = 1, \sqrt{2}, 2, 2\sqrt{2}$ with sample $k = (1, 0), (1, 1), (2, 0), (2, 2)$, the kernels are four-dimensional (Figure 4). (When $k_c = \sqrt{5}$, the kernel is eight-dimensional.)

It is also well-known that the non-linear analysis based on $\mathbf{D}_4 \times \mathbf{T}^2$ symmetry for such four-dimensional bifurcations, which are called *modes*, generically leads to two kinds of steady states: stripes and squares. Near bifurcation the pattern associated to *stripes* is just the level curves of a plane wave (one $z_k = 1$ and all other $z_k = 0$ in (1.5)) and the patten associated with *squares* is the level curves of the function in (1.5) where all $z_k = 1$. Note that stripes are horizontal when $k_c = 1, 2$ and diagonal when $k_c = \sqrt{2}, 2\sqrt{2}$. It is the horizontal stripes that occur in the simulations in Figure 3. We will show later that diagonal stripes never satisfy NBC. Squares are shown in Figure 2; we call these squares $(2, 0)$ and squares $(2, 2)$, respectively. Note the close resemblance of these patterns with the patterns obtained by numerical simulation in the first and fourth pictures in Figure 1.

Bifurcations to single modes with $\mathbf{D}_4 \times \mathbf{T}^2$ symmetry have often been studied (cf 17,19–21). Various mode interactions with $\mathbf{D}_4 \times \mathbf{T}^2$ symmetry have been studied previously, mostly by Crawford [16]. Proctor and Matthews [22] studied the $(1, 0)$ – $(1, 1)$ mode interaction which is equivalent to, the $(2, 0)$ – $(2, 2)$ mode interaction. In particular, they used the $(1, 0)$ – $(1, 1)$ interaction to explain the existence of a planform with square symmetry, observed both in numerical and laboratory experiments on non-Boussinesq convection, which has upflow in isolated plumes and downflow in connected sheets. Our study of this mode interaction will consider the effects of NBC and also parameter regimes different from those in [22].

1.6. The main results

We will show that there are paths in the parameter plane of an unfolding of the co-dimension bifurcation where the steady state $(2, 0)$ and $(2, 2)$ modes interact. Specifically, we determine the regions where equilibria and periodic orbits exist and are stable (Figures 5 and 6). By tracing paths in the parameter plane, we create bifurcation diagrams that show the equilibria and periodic orbits of these systems as time t_0 varies (Figure 7). We have found that a generic continuous transition can occur between two types of squares (Figure 5). Also, the transition between squares and stripes can generically occur either via steady states and time-periodic states (Figure 7) or via a jump (Figure 6 (right)).

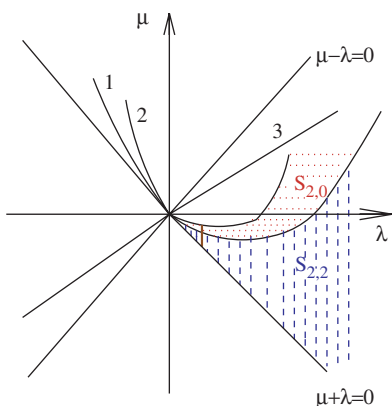


Figure 5. Regions in $\lambda\mu$ -plane of stable squares. Note: $S_{2,0}$ (horizontal dotted lines); stable squares $S_{2,2}$ (vertical dashed lines) for the non-degeneracy conditions given by (5.4); 1=steady-state bifurcation curve; 2=Hopf bifurcation curve; 3=line $\mu(\delta - \beta) + \lambda(\delta + \beta) = 0$. Thick line path parameterized by μ for fixed $\lambda > 0$ shows continuous transition from stable squares $S_{2,2}$ to stable squares $S_{2,0}$.

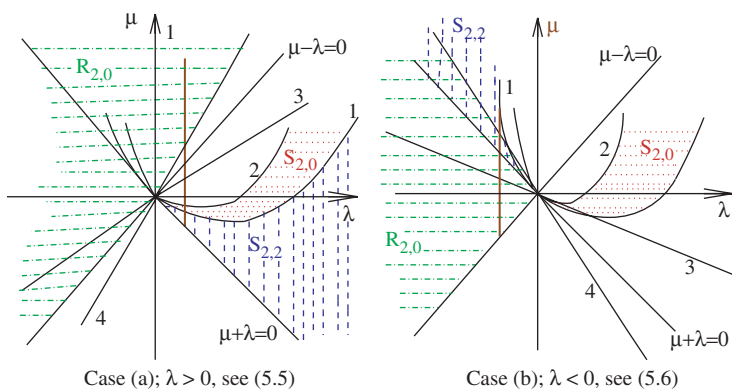


Figure 6. Regions in $\lambda\mu$ -plane of stable $S_{2,2}$ squares. Notes: (vertical dashed lines), stable $R_{2,0}$ stripes (horizontal dash-dotted lines) and stable $S_{2,0}$ squares (horizontal dotted lines) for the given non-degeneracy conditions; 1 = steady-state bifurcation curve; 2 and 4 indicate Hopf bifurcation curves; 3 = line $\mu(\delta - \beta) + \lambda(\delta + \beta) = 0$. Thick lines parameterized by μ for fixed λ show transitions: (left) from stable squares $S_{2,2}$ to stable squares $S_{2,0}$ and then to stable stripes $R_{2,0}$; (right) jump bifurcation from stable stripes $R_{2,0}$ to stable squares $S_{2,2}$.

On the mathematical side, we also show that there are significant differences between the stable patterns observed in the (2, 0)–(2, 2) mode interactions in the NBC and PBC cases. For example, certain steady states that exist in PBC do not exist in NBC (diagonal stripes) and certain states that are unstable in PBC are actually stable in NBC. In the NBC problem, we see *standing waves* time-periodic solutions as stable patterns leading to stable stripes (2, 0), whereas in the PBC problem we see *wavy rolls* steady states as stable patterns leading to stable stripes (2, 0) (Figure 8).

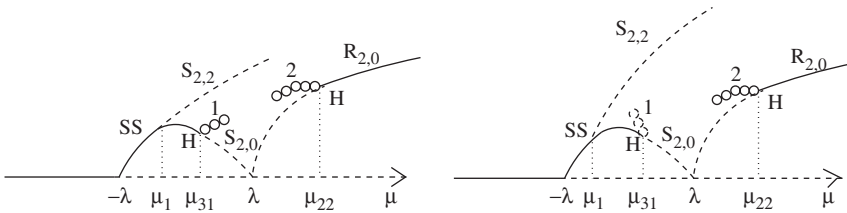


Figure 7. Possible transitions from squares (2, 2) to stripes (2, 0) via time-periodic solutions, when $\lambda > 0$ fixed for some open set of non-degeneracy conditions.

Notes: Branches 1 and 2 represent time-periodic solutions (standing waves); solid curves indicate stability; dashed curves indicate instability.

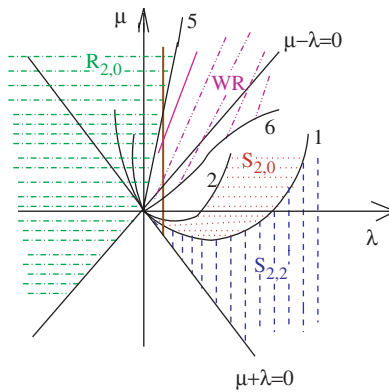


Figure 8. Regions in $\lambda\mu$ -plane of stable squares.

Notes: $S_{2,2}$ (vertical dashed lines), stable squares $S_{2,0}$ (horizontal dash-dotted lines), stable stripes $R_{2,0}$ (horizontal dotted lines), and stable WR wavy rolls $(0, z, w, -w)$ (oblique dash-double dotted lines) for some set of non-degeneracy conditions; 1 and 5 indicate steady-state bifurcation curves; 2 = Hopf bifurcation curve; 6 = some curve of bifurcation points. The thick line parameterized by μ for fixed $\lambda > 0$ shows transition from stable squares $S_{2,2}$ to stable squares $S_{2,0}$, then to a region of other solutions (which we do not investigate here), followed by stable WR wavy rolls, leading to stable stripes $R_{2,0}$ for some set of non-degeneracy conditions.

1.7. Outline of article

Our article is organized as follows. In Section 2, we recall known results about mode (2, 0) and mode (2, 2) in the PBC problem and restrict them to the NBC problem using the symmetry constraint imposed by NBC.

In Section 3, we study the PBC problem on the fixed square domain $[0, 1] \times [0, 1]$. Namely, we use the group-theoretic approach to study the (2, 0) and (2, 2) mode interaction in steady state bifurcation problems with $\mathbf{D}_4 \times \mathbf{T}^2$ symmetry. We use the normal form for the $\mathbf{D}_4 \times \mathbf{T}^2$ -equivariant vector field on $\mathbf{C}^2 \times \mathbf{C}^2$ to determine the primary branches in the PBC problem. The possible symmetries of the states are described by the isotropy lattice, and the corresponding fixed-point subspaces are determined. The primary branches of squares (2, 2), stripes (2, 2) and stripes (2, 0) occur in one-dimensional subspaces, while the primary branch of squares (2, 2) belongs to a two-dimensional subspace.

In Section 4, using isotypic decompositions, we compute the eigenvalues along the primary branches of squares (2, 2) and stripes (2, 0), as well as the stability conditions and the points of possible steady state bifurcation and Hopf bifurcation. We do not investigate the primary branch of stripes (2, 2) because it does not satisfy NBC.

Along the primary branch of squares (2, 2), we can have two types of steady state bifurcation leading to steady states with different symmetries. Only one of these steady state bifurcations can occur if we restrict to the fixed-point subspace given by NBC.

Along the primary branch of stripes (2, 0), we can have a steady state bifurcation and a Hopf bifurcation leading to time-periodic *standing waves* solutions. However, only the Hopf bifurcation can occur if we restrict to the fixed-point subspace given by NBC.

In Section 5, we restrict the previous results to the fixed-point subspace given by NBC. We show here that generic continuous transitions from squares (2, 0) to squares (2, 2) and transitions from squares (2, 2) to stripes (2, 0) (via a jump or via steady states and time-periodic states) are possible. Moreover, we determine the open sets of non-degeneracy conditions involving the coefficients of second- and third-order terms of the $\mathbf{D}_4 \times \mathbf{T}^2$ -equivariant vector field for which these situations occur. We also discuss differences between the NBC and PBC problems.

Two appendices are included. In Appendix 1, we discuss the third-order truncated normal form of the $\mathbf{D}_4 \times \mathbf{T}^2$ -equivariant vector field in the (2, 0) and (2, 2)-mode interaction. In Appendix 2, we show in detail how to find the eigenvalues of the Jacobian DF along the relevant branches.

2. Modes (2, 0) and (2, 2)

As noted in (1.5), the kernels of linearizations of the PBC problem at single-mode bifurcations are determined by symmetry. In particular, modes $(k, 0)$ and (k, k) correspond to four-dimensional kernels, which we identify with \mathbf{C}^2 . In this section we recall results of Crawford [18,20] that show that the bifurcation structure for these two modes are identical in the PBC problem but are quite different in the NBC problem. In particular, (diagonal) stripes exist for PBC in the (2, 2)-mode but not in the NBC problem.

We denote the coordinates of \mathbf{C}^2 for the $(k, 0)$ -mode by (z_1, z_2) , where the kernel of the linearization is identified with

$$z_1 e^{2k\pi i x} + z_2 e^{2k\pi i y} + \text{c.c.} \quad (2.1)$$

where c.c. indicates the complex conjugate. We denote the coordinates of \mathbf{C}^2 for the (k, k) -mode by (w_1, w_2) , where the kernel of the linearization is identified with

$$w_1 e^{2k\pi i(x+y)} + w_2 e^{2k\pi i(x-y)} + \text{c.c.} \quad (2.2)$$

It is straightforward to compute the action of $\mathbf{D}_4 \times \mathbf{T}^2$ on the coordinates of these kernels. Recall that a group element γ acting on $(x, y) \in \mathbf{R}^2$, acts on a function $f(x, y)$ by

$$(\gamma \cdot f)(x, y) = f(\gamma^{-1}(x, y))$$

For example, let $(\theta_1, \theta_2) \in \mathbf{T}^2$ be a translation. Then this group element acts on the eigenfunction (2.1) by

$$\begin{aligned} (\theta_1, \theta_2)(z_1 e^{2k\pi i x} + z_2 e^{2k\pi i y} + \text{c.c.}) &= z_1 e^{2k\pi i(x-\theta_1)} + z_2 e^{2k\pi i(y-\theta_2)} + \text{c.c.} \\ &= (e^{-2k\pi i\theta_1} z_1) e^{2k\pi i x} + (e^{-2k\pi i\theta_2} z_2) e^{2k\pi i y} + \text{c.c.} \end{aligned}$$

Table 1. Action on modes (2, 0) and (2, 2), where $\theta_1, \theta_2 \in [0, 1)$ and ξ, η are defined in (1.4).

$\mathbf{D}_4 \times \mathbf{T}^2$	(2, 0) Mode	(2, 2) Mode
1	(z_1, z_2)	(w_1, w_2)
ξ	(z_2, \bar{z}_1)	(\bar{w}_2, w_1)
ξ^2	(\bar{z}_1, \bar{z}_2)	$(\overline{(w_1, w_2)})$
ξ^3	(\bar{z}_2, z_1)	(w_2, \bar{w}_1)
η	(\bar{z}_1, z_2)	$(\overline{(w_2, w_1)})$
$\eta\xi$	(\bar{z}_2, \bar{z}_1)	(\bar{w}_1, w_2)
$\eta\xi^2$	(z_1, \bar{z}_2)	(w_2, w_1)
$\eta\xi^3$	(z_2, z_1)	(w_1, \bar{w}_2)
(θ_1, θ_2)	$(e^{-4\pi i\theta_1} z_1, e^{-4\pi i\theta_2} z_2)$	$(e^{-4\pi i(\theta_1+\theta_2)} w_1, e^{-4\pi i(\theta_1-\theta_2)} w_2)$

It follows that we can write the action of (θ_1, θ_2) on the coordinates (z_1, z_2) by

$$(\theta_1, \theta_2)(z_1, z_2) = (e^{-2k\pi i\theta_1} z_1, e^{-2k\pi i\theta_2} z_2)$$

Observe that the kernel of the action of $\mathbf{D}_4 \times \mathbf{T}^2$ on \mathbf{C}^2 in the $(k, 0)$ mode is the subgroup $\langle\langle (1/k, 0), (0, (1/k)) \rangle\rangle$, where $\langle \dots \rangle$ indicates the group generated by the listed group elements. After dividing by this kernel, we see that the group action of $\mathbf{D}_4 \times \mathbf{T}^2$ on \mathbf{C}^2 reduces to the case $k = 1$.

A similar observation can be made in the (k, k) mode. Here the action of (θ_1, θ_2) on the coordinates $(w_1, w_2) \in \mathbf{C}^2$ is

$$(\theta_1, \theta_2)(w_1, w_2) = (e^{-2k\pi i(\theta_1+\theta_2)} w_1, e^{-2k\pi i(\theta_1-\theta_2)} w_2)$$

Thus, the kernel of the action on \mathbf{C}^2 in the (k, k) mode is the subgroup $\langle\langle (1/2k, 1/2k), (1/2k, -(1/2k)) \rangle\rangle$. After dividing by this kernel, we see that this action on \mathbf{C}^2 also reduces to the case $k = 1$.

For ease of comparison with the numerical simulations, we phrase our results in the case when $k = 2$. The action of $\mathbf{D}_4 \times \mathbf{T}^2$ on the mode amplitudes for the (2, 0)-mode and the (2, 2)-mode is given in Table 1.

2.1. Modes (2, 0) and (2, 2) in PBC

As discussed in Section 1, we are primarily interested in the analysis of mode interactions (2, 0) and (2, 2) that come from NBC bifurcations. In this section and the next we build up to the analysis of this co-dimension two bifurcation by recalling results about co-dimension one single-mode PBC and NBC bifurcations.

We now show that each of these PBC co-dimension one bifurcations lead to two branches of solutions (squares and stripes). To do this we list the isotropy subgroups and their corresponding fixed-point subspaces, and the equivariant functions for each bifurcation. Recall:

Definition 2.1: (a) A subgroup $\Sigma \subset \mathbf{D}_4 \times \mathbf{T}^2$ is an *isotropy subgroup* if there exists an $z \in \mathbf{C}^2$ for which $\Sigma = \Sigma_z$, where

$$\Sigma_z = \{\gamma \in \mathbf{D}_4 \times \mathbf{T}^2 : \gamma z = z\}.$$

Table 2. Stripes and squares in mode (2, 0) with PBC.

Nomenclature	Isotropy subgroup Σ	Fix(Σ)	dim (Fix(Σ))
	$\mathbf{D}_4 \times \mathbf{T}^2$	$\{(0, 0)\}$	0
Stripes (2, 0)	$R_{2,0} \equiv \langle \eta, \xi^2, (\theta_1, 0), (0, \frac{1}{2}) \rangle$	$\{(0, z) : z \in \mathbf{R}\}$	1
Squares (2, 0)	$S_{2,0} \equiv \mathbf{D}_4 \times \langle (0, \frac{1}{2}), (\frac{1}{2}, 0) \rangle$ $\langle \eta, \xi^2, (0, \frac{1}{2}), (\frac{1}{2}, 0) \rangle$	$\{(z, z) : z \in \mathbf{R}\}$ $\{(z_1, z_2) : z_1, z_2 \in \mathbf{R}\}$	1 2

Table 3. Stripes and squares in mode (2, 2) with PBC.

Nomenclature	Isotropy subgroup Σ	Fix (Σ)	dim (Fix(Σ))
	$\mathbf{D}_4 \times \mathbf{T}^2$	$\{(0, 0)\}$	0
Stripes (2, 2)	$R_{2,2} \equiv \langle \eta\xi, \xi^2, (\theta_1, \theta_1), (0, \frac{1}{2}) \rangle$	$\{(0, w) : w \in \mathbf{R}\}$	1
Squares (2, 2)	$S_{2,2} \equiv \mathbf{D}_4 \times \langle (0, \frac{1}{2}), (\frac{1}{4}, \frac{1}{4}) \rangle$ $\langle \eta\xi, \xi^2, (0, \frac{1}{2}), (\frac{1}{4}, \frac{1}{4}) \rangle$	$\{(w, w) : w \in \mathbf{R}\}$ $\{(w_1, w_2) : w_1, w_2 \in \mathbf{R}\}$	1 2

(b) The *fixed-point subspace* of a subgroup Σ is

$$\text{Fix}(\Sigma) = \{z \in \mathbf{C}^2 : \gamma z = z, \text{ for all } \gamma \in \Sigma\}.$$

(c) A vector field $f: \mathbf{C}^2 \rightarrow \mathbf{C}^2$ is $\mathbf{D}_4 \times \mathbf{T}^2$ -equivariant if

$$f(\gamma z) = \gamma f(z)$$

for all $\gamma \in \mathbf{D}_4 \times \mathbf{T}^2$ and $z \in \mathbf{C}^2$.

The isotropy subgroups and their corresponding fixed-point subspaces for the (2, 0) and (2, 2)-modes in PBC are presented in Tables 2 and 3, respectively. They are easy to obtain using the group actions defined in Table 1. Note that we classify the isotropy subgroups of $\mathbf{D}_4 \times \mathbf{T}^2$ by conjugacy classes, since $\Sigma_{\gamma z} = \gamma \Sigma_z \gamma^{-1}$ for any $\gamma \in \mathbf{D}_4 \times \mathbf{T}^2$.

Next we write the general form for the $\mathbf{D}_4 \times \mathbf{T}^2$ -equivariant bifurcation problem (an equivariant vector field that depends on a bifurcation parameter λ) up to third-order. The (2, 0)-mode bifurcation problem $f: \mathbf{C}^2 \times \mathbf{R} \rightarrow \mathbf{C}^2$ has the form

$$\begin{aligned} f^1(z_1, z_2, \lambda) &= z_1(\lambda + B_1|z_1|^2 + C_1|z_2|^2) + \dots \\ f^2(z_1, z_2, \lambda) &= z_2(\lambda + B_1|z_2|^2 + C_1|z_1|^2) + \dots \end{aligned} \tag{2.3}$$

where $f = (f^1, f^2)$ and $B_1, C_1 \in \mathbf{R}$. The (2, 2)-mode bifurcation problem $g: \mathbf{C}^2 \times \mathbf{R} \rightarrow \mathbf{C}^2$ has the form

$$\begin{aligned} g^1(w_1, w_2, \lambda) &= w_1(\lambda + C_2|w_1|^2 + D_2|w_2|^2) + \dots \\ g^2(w_1, w_2, \lambda) &= w_2(\lambda + C_2|w_2|^2 + D_2|w_1|^2) + \dots \end{aligned} \tag{2.4}$$

where $g = (g^1, g^2)$ and $C_2, D_2 \in \mathbf{R}$. In each case we rescaled the coefficient of λ to be 1.

Since fixed-point subspaces are flow-invariant for every equivariant vector field, we can find branches of squares by restricting to the subspaces (z, z) and (w, w) (where $z, w \in \mathbf{R}$)

Table 4. Primary branches for (2, 0) and (2, 2) modes in NBC.

Isotropy subgroup Σ	$f _{\text{Fix}(\Sigma)}=0$	Primary branches (NBC)	Eigenvalues (NBC)
Panel A: (2, 0)-mode in NBC			
$S_{2,0}$	$f^1=0$ at (z, z, λ)	$\lambda = -(B_1 + C_1)z^2 + \dots$	$2(B_1 + C_1)z^2$
$R_{2,0}$	$f^2=0$ at $(0, z, \lambda)$	$\lambda = -B_1z^2 + \dots$	$+\dots 2(B_1 - C_1)z^2 + \dots$ $2B_1z^2 + \dots (C_1 - B_1)z^2 + \dots$
Panel B: (2, 2)-mode in NBC			
$S_{2,2}$	$f^3=0$ at (w, w, λ)	$\lambda = -(C_2 + D_2)w^2 + \dots$	$2(C_2 + D_2)w^2 + \dots$

and branches of stripes by restricting to the subspaces $(0, z)$ and $(0, w)$ (where $z, w \in \mathbf{R}$). Moreover, since the forms of f and g are the same, so are the stability analyses of solutions.

2.2. Modes (2, 0) and (2, 2) in NBC

We will show that NBC and PBC bifurcations are the same in the (2, 0)-mode and are quite different in the (2, 2)-mode. This happens because NBC solutions are solutions to the PBC problem that satisfy the NBC symmetry constraint (1.2) and stripes do not satisfy this constraint.

From Table 1 we see that

$$\text{Fix}(\langle \eta, \xi^2 \rangle) = \{(z_1, z_2) : z_1, z_2 \in \mathbf{R}\} \quad \text{for (2, 0)-mode}$$

is two-dimensional and

$$\text{Fix}(\langle \eta, \xi^2 \rangle) = \{(w, w) : w \in \mathbf{R}\} \quad \text{for (2, 2)-mode}$$

is one-dimensional. It follows that stripes and squares appear in the NBC (2, 0)-mode, whereas only squares appear in the NBC (2, 2)-mode bifurcation. To verify this point, observe that any solution conjugate to stripes has the form $(0, w)$ or $(w, 0)$, where $w \in \mathbf{C}$, and none of these points belong to $\{(w, w) : w \in \mathbf{R}\}$.

The details about the branches bifurcating from trivial solution are summarized in Table 4 and (Panels A and B). The bifurcation diagrams for NBC are shown in Figures 9 and 10. These figures are obtained by restricting the $\mathbf{D}_4 \times \mathbf{T}^2$ -equivariant bifurcation problems given by (2.3) and (2.4) to $\text{Fix}(\langle \eta, \xi^2 \rangle)$.

3. (2, 0)–(2, 2) Mode interaction in PBC

In this section we review the study of (2, 0)–(2, 2) mode interaction steady state bifurcation problems with $\mathbf{D}_4 \times \mathbf{T}^2$ -symmetry (the PBC problem). Most results stated here can be found in Proctor and Matthews [22].

The (2, 0)–(2, 2) steady state mode interaction bifurcation problem is a co-dimension two linear degeneracy that corresponds to modes (2, 0) and (2, 2) going unstable simultaneously as two parameters are varied. Such degeneracies are interesting because non-linear terms couple the modes to create states whose behaviour is more complicated than is expected from the modes individually. These new states are said to be produced by *mode interaction*.

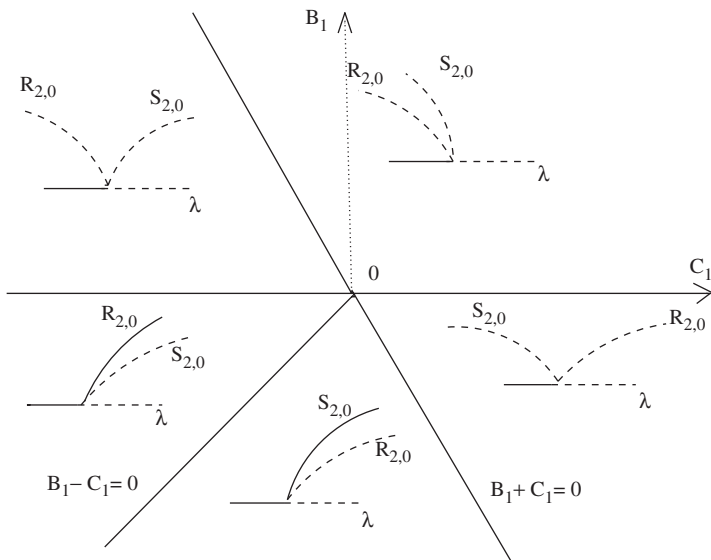


Figure 9. Bifurcation diagram for (2,0)-mode in NBC.
 Note: unstable (dashed lines); stable (solid lines); $R_{2,0}$ = stripes (2, 0); $S_{2,0}$ = squares (2, 0).



Figure 10. Bifurcation diagrams for (2,2)-mode in NBC.
 Note: unstable (dashed lines); stable (solid lines); $S_{2,2}$ = squares (2, 2).

We denote the coordinates of $\mathbf{C}^2 \times \mathbf{C}^2$ by (z_1, z_2, w_1, w_2) . The action of $\mathbf{D}_4 \times \mathbf{T}^2$ on $\mathbf{C}^2 \times \mathbf{C}^2$ is given in Table 1. The kernel of the action is the subgroup $\langle (0, 1/2), (1/2, 0) \rangle$.

We discuss the isotropy lattice and the corresponding fixed-point subspaces in Section 3.1. The truncated normal form up to third-order terms of a $\mathbf{D}_4 \times \mathbf{T}^2$ -equivariant vector field is given in Section 3.2. We use it to determine the primary branches in Section 3.3. We justify this truncation by noting that all the directions of the branching and their stabilities computed in Sections 3 and 4 are determined by third-order terms.

3.1. Isotropy subgroups and fixed-point subspaces

The conjugacy classes of isotropy subgroups of the action of $\mathbf{D}_4 \times \mathbf{T}^2$ on \mathbf{C}^4 can be computed using Table 1. The results are listed in Table 5 and Figure 11. Note that the subgroup associated to NBC is an isotropy subgroup and its fixed-point subspace is the three-dimensional subspace

$$\mathcal{N} \equiv \text{Fix}(\langle \eta, \xi^2 \rangle) = \{(z_1, z_2, w, w) : z_1, z_2, w \in \mathbf{R}\}.$$

Table 5. Fixed-point subspaces in PBC.

Nomenclature	Isotropy Σ	Fix(Σ)	dim(Fix(Σ))
Squares (2, 2)	$S_{2,2} = \mathbf{D}_4 \times \langle (\frac{1}{4}, \frac{1}{4}) \rangle$	$\{(0, 0, w_1, w_1) : w_1 \in \mathbf{R}\}$	1
Stripes (2, 2)	$R_{2,2} = \langle \eta\xi, \xi^2, (\theta_1, \theta_1) \rangle$	$\{(0, 0, 0, w_1) : w_1 \in \mathbf{R}\}$	1
Squares (2, 0)	$S_{2,0} = \mathbf{D}_4$	$\{(z_1, z_1, w_1, w_1) : z_1, w_1 \in \mathbf{R}\}$	2
Stripes (2, 0)	$R_{2,0} = \langle \eta, \xi^2, (\theta_1, 0) \rangle$	$\{(0, z_2, 0, 0) : z_2 \in \mathbf{R}\}$	1
(5)	$\langle \eta\xi, \xi^2, (\frac{1}{4}, \frac{1}{4}) \rangle$	$\{(0, 0, w_1, w_2) : w_1, w_2 \in \mathbf{R}\}$	2
(6)	$\langle \eta, \xi^2 \rangle$	$\{(z_1, z_2, w_1, w_1) : z_1, z_2, w_1 \in \mathbf{R}\}$	3
(7)	$\langle \eta\xi, \xi^2 \rangle$	$\{(z_1, z_1, w_1, w_2) : z_1, w_1, w_2 \in \mathbf{R}\}$	3
(8)	$\langle \xi^2 \rangle$	$\{(z_1, z_2, w_1, w_2) : z_1, z_2, w_1, w_2 \in \mathbf{R}\}$	4
(9)	$\langle \eta \rangle$	$\{(z_1, z_2, w_1, w_1) : z_1 \in \mathbf{R}, z_2, w_1 \in \mathbf{C}\}$	5
	1	$\mathbf{C}^2 \times \mathbf{C}^2$	8

Note: The kernel $\langle (0, 1/2), (1/2, 0) \rangle$ is not shown in the isotropy subgroups.

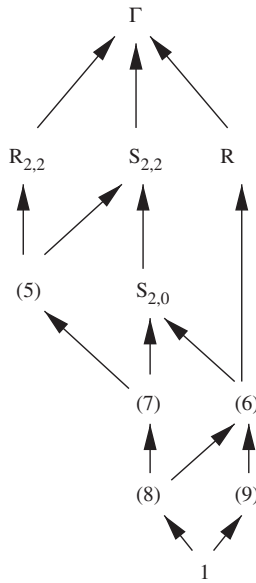


Figure 11. Isotropy lattice in PBC; $\Gamma = \mathbf{D}_4 \times \mathbf{T}^2$.

3.2. The normal form

Matthews and Proctor [22] obtained the normal form truncated up to third-order for the $\mathbf{D}_4 \times \mathbf{T}^2$ -equivariant vector field. In Appendix 1 we re-derive this truncated normal form. The general normal form can also be obtained, but in Sections 3 and 4 we work only with the truncated normal form up to third-order terms given by (3.1).

The steady state/steady state mode interaction is a co-dimension two bifurcation problem with two parameters λ and μ , such that

$$F(0, 0, \lambda, \mu) = 0 \quad \text{and} \quad (DF)_{(0,0,0,0)} = 0.$$

The $\mathbf{D}_4 \times \mathbf{T}^2$ -equivariant bifurcation problem truncated at third-order is given by

$$\begin{aligned}
 f^1(z_1, z_2, w_1, w_2, \lambda, \mu) &= (-\lambda + \mu)z_1 + A_1(z_2w_2 + \overline{z_2}w_1) + E_1\overline{z_1}w_1w_2 \\
 &\quad + [B_1|z_1|^2 + C_1|z_2|^2 + D_1(|w_1|^2 + |w_2|^2)]z_1 \\
 f^2(z_1, z_2, w_1, w_2, \lambda, \mu) &= f^1(z_2, z_1, w_1, \overline{w_2}, \lambda, \mu) \\
 g^1(z_1, z_2, w_1, w_2, \lambda, \mu) &= (\lambda + \mu)w_1 + A_2z_1z_2 + E_2(z_1^2\overline{w_2} + z_2^2w_2) \\
 &\quad + [B_2(|z_1|^2 + |z_2|^2) + C_2|w_1|^2 + D_2|w_2|^2]w_1 \\
 g^2(z_1, z_2, w_1, w_2, \lambda, \mu) &= g^1(z_1, \overline{z_2}, w_2, w_1, \lambda, \mu),
 \end{aligned} \tag{3.1}$$

where $F = (f^1, f^2, g^1, g^2)$ and $A_1, B_1, C_1, D_1, E_1, A_2, B_2, C_2, D_2, E_2$ are real constants. In this normal form we have chosen the parameters so that μ is the bifurcation parameter and λ is the splitting parameter. The roles of these parameters are best understood by observing the changes in stability of the trivial solution. The Jacobian of F at $(0, 0, \lambda, \mu)$ in block form is

$$(DF)_{(0,0,\lambda,\mu)} = \begin{pmatrix} (-\lambda + \mu) & I0 \\ 0 & (\lambda + \mu)I \end{pmatrix}.$$

Hence, the eigenvalues of $(DF)_{(0,0,\lambda,\mu)}$ are $-\lambda + \mu$ and $\lambda + \mu$, each with algebraic multiplicity 4. The trivial solution loses stability first at either $\mu = -\lambda$ or $\mu = \lambda$ depending on the sign of λ .

3.3. Primary branches

The details about the primary branches in PBC are summarized in Table 6. The Equivariant Branching Lemma [19] guarantees the existence of branches of solutions corresponding to each one-dimensional fixed-point subspace. In this mode interaction there are three such primary branches, and they are listed in Table 5 (along with their isotropy subgroups): squares (2, 2) ($S_{2,2}$), stripes (2, 2) ($R_{2,2}$), and stripes (2, 0) ($R_{2,0}$).

A more interesting fact is the existence of a primary branch of squares (2, 0) in the two-dimensional submaximal subspace $\text{Fix}(\mathbf{D}_4)$. This *non-axial* branch is discussed next.

Table 6. Primary branches in PBC.

	Σ	$f _{\text{Fix}(\Sigma)} = 0$	Primary branches
$S_{2,2}$	$\mathbf{D}_4 \times \langle (1/4, 1/4) \rangle$	$g^1(0, 0, w, w, \lambda, \mu) = 0$	$\mu = -\lambda - \delta w^2 + \dots$
$R_{2,2}$	$\langle \eta\xi, \xi^2, (\theta_1, \theta_1) \rangle$	$g^2(0, 0, 0, w, \lambda, \mu) = 0$	$\mu = -\lambda - C_2 w^2 + \dots$
$R_{2,0}$	$\langle \eta, \xi^2, (\theta_1, 0) \rangle$	$f^1(z, 0, 0, 0, \lambda, \mu) = 0$	$\mu = \lambda - B_1 z^2 + \dots$
$S_{2,0}$	\mathbf{D}_4	$f^1/z = 0, g^1 = 0$ at $(z, z, w, w, \lambda, \mu)$	if $A_1 A_2 \neq 0$

Note: Note that the kernel $\langle (0, 1/2), (1/2, 0) \rangle$ is not recorded in the isotropy subgroups. Here $z, w \in \mathbf{R}$.

3.3.1. Primary branch of squares $(2, 0)$ in $\text{Fix}(D_4)$

Observe that when restricted to $z = z_2 = z_1 \in \mathbf{R}$ and $w = w_2 = w_1 \in \mathbf{R}$, the equation

$$f^1/z = 0 \quad \text{and} \quad g^1 = 0$$

are

$$\begin{aligned} -\lambda + \mu + 2A_1w + \alpha z^2 + \beta w^2 &= 0 \\ (\lambda + \mu)w + A_2z^2 + 2\gamma z^2w + \delta w^3 &= 0. \end{aligned} \tag{3.2}$$

where

$$\alpha = B_1 + C_1, \quad \beta = 2D_1 + E_1, \quad \gamma = B_2 + E_2 \quad \text{and} \quad \delta = C_2 + D_2. \tag{3.3}$$

Let $u = z^2$ and rewrite (3.2) as

$$\begin{aligned} -\lambda + \mu + 2A_1w + \alpha u + \beta w^2 &= 0 \\ (\lambda + \mu)w + A_2u + 2\gamma uw + \delta w^3 &= 0. \end{aligned} \tag{3.4}$$

When $A_1A_2 \neq 0$, we can use the Implicit Function Theorem to solve (3.4) for $u = U(\mu, \lambda)$ and $w = W(\mu, \lambda)$, where $U(0, 0) = W(0, 0) = 0$. Thus, when λ is fixed and near zero, a curve of solutions to (3.4) is given by $(U(\cdot, \lambda), W(\cdot, \lambda))$. However, only those μ for which $U(\mu, \lambda) \geq 0$ are actually solutions to (3.2), that is, squares $(2, 0)$ solutions $(S_{2,0})$.

To understand the possible bifurcation diagrams of squares $(2, 0)$ solutions as μ varies, we begin by setting $\lambda = 0$. Implicit differentiation of (3.4) leads to

$$W_\mu(0, 0) = -\frac{1}{2A_1} \quad U_\mu(0, 0) = 0 \quad U_{\mu\mu}(0, 0) = \frac{1}{A_1A_2}$$

So, if $A_1A_2 < 0$ there are no solutions to (3.2) and when $A_1A_2 > 0$, there are two transcritical branches of squares $(2, 0)$

$$(z, w) = \left(\frac{1}{\sqrt{2A_1A_2}}, -\frac{1}{2A_1}\right)\mu + \dots \quad \text{and} \quad (z, w) = \left(-\frac{1}{\sqrt{2A_1A_2}}, -\frac{1}{2A_1}\right)\mu + \dots,$$

and these two branches are related by the symmetry $(z, w) \mapsto (-z, w)$. The bifurcation diagrams at $\lambda = 0$ are given in Figure 12. Other bifurcation diagrams are also possible.

Next we determine the structure of solution branches when $\lambda \neq 0$. This is most simply done by computing the region in the (μ, λ) plane where $U \geq 0$. The Taylor expansion of U begins with quadratic terms in μ and λ . Specifically, implicit differentiation yields

$$U_\lambda(0, 0) = 0 \quad U_{\mu\mu}(0, 0) = \frac{1}{A_1A_2} = -U_{\lambda\lambda}(0, 0) \quad U_{\lambda\mu}(0, 0) = 0.$$

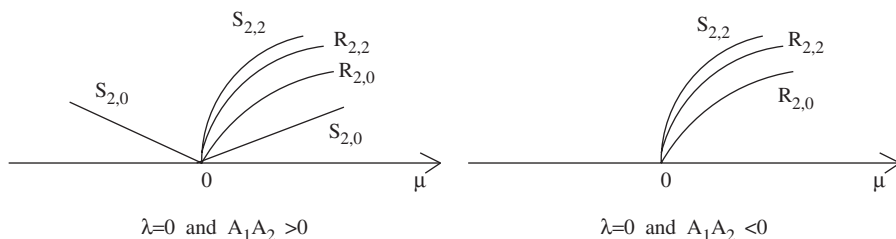


Figure 12. Sample mode interaction bifurcation diagrams.

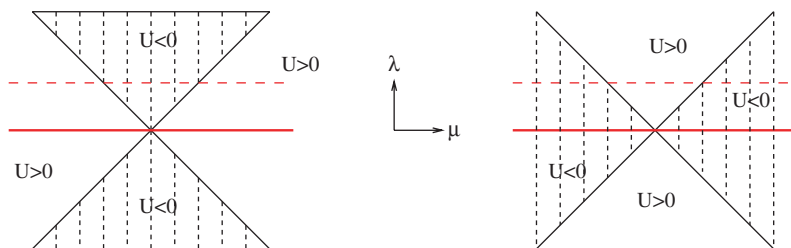


Figure 13. $U > 0$ for (μ, λ) in white region; $U < 0$ for (μ, λ) in hatched region. Note: (Left) $A_1 A_2 > 0$; (right) $A_1 A_2 < 0$.

so that

$$U(\mu, \lambda) = \frac{1}{2A_1 A_2} (\mu^2 - \lambda^2) + \dots$$

It follows from the singularity theory with a distinguished parameter approach to bifurcation theory [23] that there is a change of coordinates $(\mu, \lambda) \rightarrow (\mu', \lambda')$ with μ' depending only on μ such that in the new coordinates

$$U(\mu, \lambda) = \text{sgn}(A_1 A_2) (\mu'^2 - \lambda'^2),$$

where, to simplify notation, we delete the primes on μ' and λ' .

Hence, the region of the plane where $U \geq 0$ is the region given in Figure 13 with two bounding curves defined by $U(\mu, \lambda) = 0$. Observe that $\mu = \lambda$ and $u = w = 0$ is a solution to (3.4). Uniqueness of solutions obtained by the Implicit Function Theorem implies that $U(\mu, \mu) = 0 = W(\mu, \mu)$. Hence, the solution of (3.4) that corresponds to the line $\mu = \lambda$ is the trivial solution. Conversely, $u = w = 0$ implies that $\mu = \lambda$. Hence, the solution to (3.4) that corresponds to the other branch of $U(\mu, \lambda) = 0$ is *not* the trivial solution. Indeed, $U = 0$ and $W \neq 0$ at this bifurcation. From Table 6 we see that such solutions are of type squares (2, 2).

When $A_1 A_2 > 0$ and $\lambda > 0$ (represented by the horizontal dashed line in Figure 13 (left)), observe that there are two solution branches as μ varies – with the first branch ending at approximately $\mu = -|\lambda|$ and the second branch beginning at $\mu = |\lambda|$. The first branch ends at a squares (2, 2) solution ($S_{2,2}$) and the second branch begins at a trivial solution. When $\lambda < 0$, the first branch ends at a trivial solution and the second begins at a square (2, 2) solution. The symmetry $(z, w) \mapsto (-z, w)$ guarantees that both branches are parabolas.

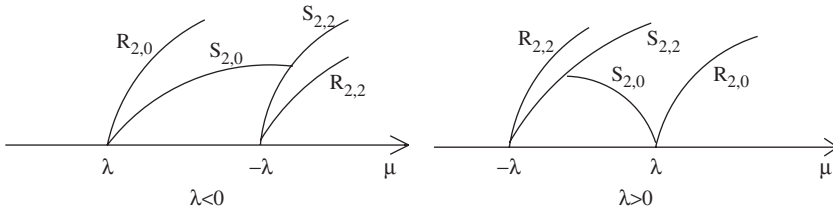


Figure 14. Bifurcation of primary branches when $A_1A_2 < 0$.

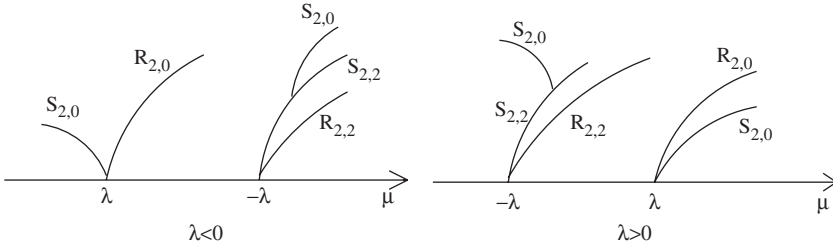


Figure 15. Bifurcation of primary branches when $A_1A_2 > 0$.

Similarly, when $A_1A_2 < 0$, the region of the plane where $U \geq 0$ is the region given in Figure 13 (right). In this case, when λ is fixed and non-zero, there is a single isola branch of squares (2, 0) solutions as μ varies that connects a trivial solution with a squares (2, 2) solution. The isola exists between λ and approximately $-\lambda$.

Possible bifurcation diagrams for $\lambda \neq 0$ showing only the primary branches and a secondary branch of the primary mode squares (2, 0) are given in Figures 14 and 15. There are other possible bifurcation diagrams.

4. Eigenvalues and secondary bifurcations in PBC

In this section we discuss *secondary bifurcations* from the primary branches of squares (2, 2) and stripes (2, 0). We do not consider stripes (2, 2), since these solutions do not appear in the NBC case. In Section 5.1 we compute the eigenvalues of the Jacobian DF along the primary branch of squares (2, 0) in the NBC problem.

The approach is standard: we track the eigenvalues of DF along the primary branches and use symmetry, in the form of isotypic components, to determine the kinds of bifurcations that can occur. The Jacobian at an equilibrium is an 8×8 matrix whose eigenvalues can be determined using symmetry. There are two restrictions on DF (see [19]). First, the isotropy subgroup corresponding to a solution decomposes \mathbf{C}^4 into isotypic components, which provide coordinates that block diagonalized DF . Second, continuous group orbits of solutions force zero eigenvalues.

In Section 4.1 we list the isotypic decomposition for the isotropy subgroups along the primary branches; see Table 7. Then, we use this information to determine the eigenvalues along these solution branches in Section 4.2 and discuss the secondary bifurcations; these results are summarized in Table 8. Part of these results were also obtained by Proctor and Matthews in [22].

Table 7. Isotypic decompositions of \mathbf{C}^4 for $S_{2,2}, R_{2,0}, S_{2,0}$.

Σ	Isotypic decomposition for Σ	$\ker(\Sigma)$ on V_i^j
$S_{2,2}$	$V_1^1 = \mathbf{R}(0, 0, 1, 1)$	$S_{2,2}$
	$V_2^1 = \mathbf{R}(1, 1, 0, 0)$	\mathbf{D}_4
	$V_3^1 = \mathbf{R}(1, -1, 0, 0)$	$\langle \eta, \xi(\frac{1}{4}, \frac{1}{4}) \rangle$
	$V_4^1 = \mathbf{R}(0, 0, 1, -1)$	$\langle \eta\xi, \xi^2, (\frac{1}{4}, \frac{1}{4}) \rangle$
	$V_5^1 = \mathbf{R}\{(0, 0, i, 0), (0, 0, 0, i)\}^*$	$\langle (\frac{1}{4}, \frac{1}{4}) \rangle$
	$V_6^1 = \mathbf{R}\{(i, 0, 0, 0), (0, i, 0, 0)\}$	1
$R_{2,0}$	$V_1^2 = \mathbf{R}(0, 1, 0, 0)$	$R_{2,0}$
	$V_2^2 = \mathbf{R}(0, i, 0, 0)^*$	$\langle \eta, (\theta_1, 0) \rangle$
	$V_3^2 = \{(0, 0, w, -w) : w \in \mathbf{C}\}$	1
	$V_4^2 = \{(z, 0, w, w) : z, w \in \mathbf{C}\}$	$\langle \eta\xi^2 \rangle$
$S_{2,0}$	$V_1^3 = \mathbf{R}\{(1, 1, 0, 0), (0, 0, 1, 1)\}$	$S_{2,0}$
	$V_2^3 = \mathbf{R}\{(1, -1, 0, 0), (0, 0, 1, -1)\}$	$\langle \eta, \xi^2 \rangle$
	$V_3^3 = \mathbf{R}\{(i, 0, 0, 0), (0, i, 0, 0), (0, 0, i, 0), (0, 0, 0, i)\}$	1

*Note: Indicates nullspace.

Table 8. Data for secondary bifurcations along squares $S_{2,2}$ ($(0, 0, w, w)$ with $\mu = -\lambda - \delta w^2 + \dots$) and stripes $R_{2,0}$ ($(0, z, 0, 0)$ with $\mu = \lambda - B_1 z^2 + \dots$) in PBC.

Σ	Nonzero eigenvalues (PBC)	Points of secondary bifurcation	Nondegeneracy conditions
$S_{2,2}$	$2\delta w^2 + \dots$	No bifurcation	$\delta \neq 0$
	$\mu - \lambda + 2A_1 w + \beta w^2 + \dots$	$\mu_{11} \equiv -\lambda - \frac{\delta}{A_1^2} \lambda^2 + \dots$	$\lambda A_1 > 0$
	$\mu - \lambda - 2A_1 w + \beta w^2 + \dots$	$\mu_{12} \equiv -\lambda - \frac{\delta}{A_1^2} \lambda^2 + \dots$	$\lambda A_1 < 0$
	$2(C_2 - D_2)w^2 + \dots$	No bifurcation	$C_2 \neq D_2$
	$\mu - \lambda + (2D_1 - E_1)w^2 + \dots$	$\mu_{13} \equiv -\lambda \frac{2D_1 - E_1 + \delta}{2D_1 - E_1 - \delta} + \dots$	$\lambda(2D_1 - E_1 - \delta) > 0$
$R_{2,0}$	$2B_1 z^2 + \dots$	No bifurcation	$B_1 \neq 0$
	$\mu + \lambda + (B_2 - E_2)z^2 + \dots$	$\mu_{21} \equiv \lambda \frac{-B_1 - B_2 + E_2}{B_1 - B_2 + E_2} + \dots$	$\lambda(B_1 - B_2 + E_2) > 0$
	$\text{tr} = 2\mu + (C_1 + \gamma)z^2 + \dots$ $\text{det} = -2A_1 A_2 z^2 + \dots$	$\mu_{22} \equiv \lambda \frac{C_1 + \gamma}{-2B_1 + C_1 + \gamma} + \dots$	$A_1 A_2 < 0$ $\lambda(-2B_1 + C_1 + \gamma) < 0$

Note: Steady-state bifurcations occur at $\mu_{11}, \mu_{12}, \mu_{13}, \mu_{21}$ and Hopf bifurcation occurs at μ_{22} .

4.1. Isotypic decompositions

An *isotypic component* of an isotropy subgroup Σ is the sum of all isomorphic irreducible representations of Σ in \mathbf{C}^4 . The first fact is that every isotypic component is $(DF)_z$ invariant, where the isotropy subgroup of z is Σ . The second fact is that \mathbf{C}^4 can be written

uniquely as a direct sum of isotypic components $V_1 \oplus \dots \oplus V_\ell$ for Σ . One isotypic component is standard for every isotropy subgroup, namely, $V_1 = \text{Fix}(\Sigma)$.

In Table 7 we list the isotypic decomposition of \mathbf{C}^4 for $S_{2,2}$, $R_{2,0}$, and $R_{2,0}$. We also list the nullvectors of DF that are forced by symmetry. These nullspaces are found by computing the tangent vectors to the group orbits through the solution point, which is done as follows.

$$\frac{d}{ds}(s, 0)(z_1, z_2, w_1, w_2)|_{s=0} = \frac{d}{ds}(e^{-4\pi is} z_1, z_2, e^{-4\pi is} w_1, e^{-4\pi is} w_2)|_{s=0} = -4\pi i(z_1, 0, w_1, w_2)$$

$$\frac{d}{dt}(0, t)(z_1, z_2, w_1, w_2)|_{t=0} = \frac{d}{dt}(z_1, e^{-4\pi it} z_2, e^{-4\pi it} w_1, e^{4\pi it} w_2)|_{t=0} = -4\pi i(0, z_2, w_1, -w_2).$$

4.2. Eigenvalues and bifurcations along the primary branches

Using the isotypic decompositions, we determine the eigenvalues of the Jacobian DF along the primary branches of squares (2, 2) and stripes (2, 0) in the PBC problem. This information is summarized in Table 8. In Section 5.4 we will use the eigenvalues of the Jacobian DF along the primary branches of squares (2, 2) and stripes (2, 0) in the PBC problem to show the difference between stable solutions in the NBC and PBC problems. The method of finding the eigenvalues listed in Table 8 is described in Appendix 2.

The primary branches are orbitally stable if all the eigenvalues of the Jacobian DF along the primary branches, not forced by symmetry to be zero, have negative real part. *Steady-state (SS) secondary bifurcations* occur along primary branches if one of the eigenvalues of DF is zero and *Hopf (H) secondary bifurcations* occur when there is a pair of purely imaginary eigenvalues. The information regarding possible secondary bifurcations is summarized in Table 8.

The calculations needed to obtain the information listed in Table 8 are given in Appendix 2; in particular see (A7), (A8), and (A9). Recall that the constants $\alpha, \beta, \gamma, \delta$ are defined in (3.3).

For example, steady state bifurcations can occur from the $S_{2,2}$ branch by having a zero eigenvalue in one of the isotypic components V_2^1 and V_3^1 if

$$a_2 = \mu - \lambda + 2A_1 w + \beta w^2 + \dots = 0 \quad \text{or} \quad a_3 = \mu - \lambda - 2A_1 w + \beta w^2 + \dots = 0.$$

See (B2). These two equations are equivalent to

$$a_2 a_3 = (\mu - \lambda + \beta w^2)^2 - 4A_1^2 w^2 + \dots = 0 \tag{4.1}$$

In addition, $S_{2,2}$ solutions satisfy

$$\mu + \lambda = -\delta w^2 + \dots$$

Thus, to second order in λ and μ , (4.1) has the form

$$-4 \frac{A_1^2}{\delta^2} (\mu + \lambda) + \frac{(\delta - \beta)^2}{\delta^2} \mu^2 + \frac{(\delta + \beta)^2}{\delta^2} \lambda^2 - 2 \frac{\delta^2 - \beta^2}{\delta^2} \mu \lambda + \dots = 0 \tag{4.2}$$

and there is a steady state bifurcation in one of V_2^1 and V_3^1 when $\mu = -\lambda - (\delta/A_1^2)$ (using the implicit function theorem for (4.2)). Another calculation shows that whether $a_2 = 0$ or

$a_3 = 0$ depends on the sign of $A_1\lambda$. The expansions of μ_{11} and μ_{12} to second order in λ are needed for the stability analysis of squares (2, 2) given in Section 5.

Also, a Hopf bifurcation can occur from the $R_{2,0}$ branch if

$$\text{tr} = 2\mu + (C_1 + \gamma)z^2 + \dots = 0 \quad \text{and} \quad \det = -2A_1A_2z^2 + \dots > 0.$$

Then $z^2 = -(2\mu/C_1 + \gamma) + \dots$. Substituting $\mu = \lambda - B_1z^2 + \dots$ into the expression for z^2 , it follows that $(\lambda/-2B_1 + C_1 + \gamma) < 0$. Also, $\det > 0$ implies $A_1A_2 < 0$. Substituting $z^2 = (\lambda - \mu/B_1) + \dots$ into the expression for the trace, we obtain the value of μ_{22} listed in Table 8.

5. Restriction to NBC

In the first three sections of ‘Introduction’, we restrict the PBC problem to the three-dimensional fixed-point subspace given by NBC

$$\mathcal{N} \equiv \text{Fix}((\eta, \xi^2)) = \{(z_1, z_2, w, w) : z_1, z_2, w \in \mathbf{R}\}.$$

In Section 5.4 we point out interesting differences between the PBC and NBC problems.

From (3.1), the normal form of the $\mathbf{D}_4 \times \mathbf{T}^2$ -equivariant vector field F truncated at third-order and restricted to \mathcal{N} is given by

$$\begin{aligned} f^1(z_1, z_2, w, w, \lambda, \mu) &= (-\lambda + \mu)z_1 + 2A_1z_2w + [B_1z_1^2 + C_1z_2^2 + \beta w^2]z_1 \\ f^2(z_1, z_2, w, w, \lambda, \mu) &= (-\lambda + \mu)z_2 + 2A_1z_1w + [C_1z_1^2 + B_1z_2^2 + \beta w^2]z_2 \\ g(z_1, z_2, w, w, \lambda, \mu) &= (\lambda + \mu)w + A_2z_1z_2 + [\gamma(z_1^2 + z_2^2) + \delta w^2]w, \end{aligned} \tag{5.1}$$

where $F|_{\mathcal{N}} = (f^1, f^2, g, g) : \mathcal{N} \times \mathbf{R}^2 \rightarrow \mathcal{N}$. The isotropy lattice restricted to NBC is presented in Figure 16.

We discuss the following interesting situations that occur *generically* in the restriction of the PBC problem to $\mathcal{N} \equiv \text{Fix}((\eta, \xi^2))$:

- (a) continuous transition from squares (2, 0) to squares (2, 2);

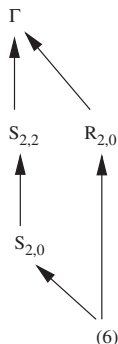


Figure 16. Isotropy lattice restricted to $\mathcal{N} \equiv \text{Fix}((\eta, \xi^2))$. Note: Subgroups are defined in Table 5.

- (b) transition via steady states and time-periodic states (standing waves) between squares (2, 2) and stripes (2, 0);
- (c) transition between squares (2, 2) and stripes (2, 0) via a jump.

We determine non-degeneracy conditions, which are valid on an open set of parameters, involving second and third-order terms of $F|_{\mathcal{N}}$ for which (a, b, c) each occur *generically* in the NBC problem. These non-degeneracy conditions can be used to construct generic reaction-diffusion systems with NBC on growing square domains that show prescribed transitions between different types of patterns, though we have not done this.

We mentioned in Section 3 that solutions on the primary branch of stripes (2, 2) ($R_{2,2}$) do not satisfy NBC. Therefore, we redisplay the bifurcation diagrams (in μ) that contain only those primary branches that do appear in the NBC bifurcation problems. See Figure 17 for the (most relevant) diagrams when $\lambda = 0$ and Figures 18 and 19 for these cases when $\lambda \neq 0$.

In Section 5.1 we discuss the data needed to find secondary bifurcations along squares (2, 2), stripes (2, 0) and squares (2, 0) in the NBC problems.

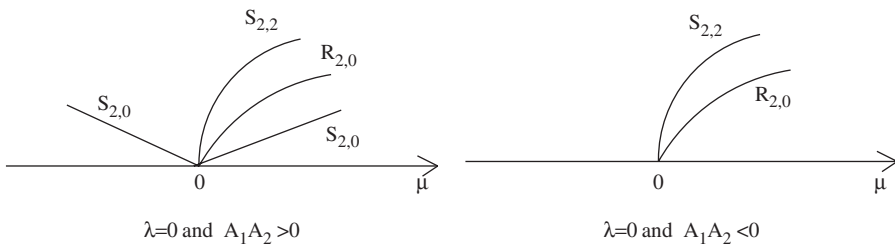


Figure 17. Restriction to NBC of PBC bifurcation diagrams in Figure 12.

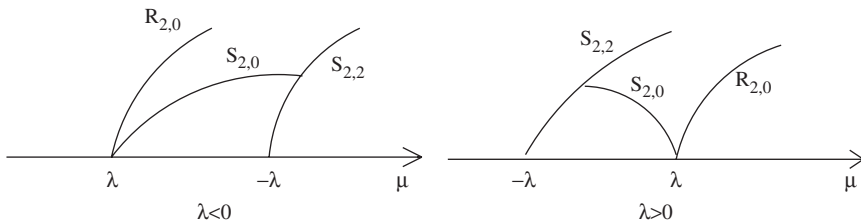


Figure 18. Restriction to NBC of PBC bifurcation diagrams in Figure 14: $A_1 A_2 < 0$.

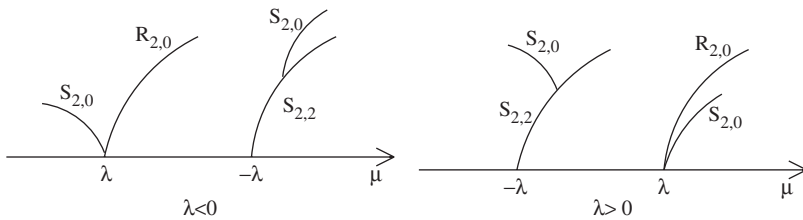


Figure 19. Restriction to NBC of PBC bifurcation diagrams in Figure 15: $A_1 A_2 > 0$.

We determine non-degeneracy conditions in Section 5.2 for which a continuous transition from squares (2, 0) to squares (2, 2) can occur (Figure 5). In Section 5.3 we determine non-degeneracy conditions for which the transitions from squares (2, 2) to stripes (2, 0) can occur via steady states and time-periodic states (see Figure 7) or via a jump (see Figure 6 (right)).

We note that the planforms of the solution branches in the NBC problem inherit the reflectional symmetry about the mid-axes of $[0, 1/2] \times [0, 1/2]$ due to the extra translational symmetries (0, 1/2) and (1/2, 0). See Figure 2.

We have already noted that stripes (2, 2) exist in PBC problems but do not exist in NBC problems. In Section 5.4 we also show the stable patterns leading to stripes (2, 0) can be *standing waves* in the NBC problem and *wavy rolls* in the PBC problem.

5.1. Secondary bifurcations in NBC

In this section, we discuss the possible secondary bifurcations in the NBC problem along the primary branches of squares (2, 2), stripes (2, 0) and squares (2, 0), together with the eigenvalues of $DF|_{\mathcal{N}}$ along these branches.

In Table 9 the action of $\langle \xi, (0, 1/4), (1/4, 1/4) \rangle$ on $\mathcal{N} \equiv \text{Fix}(\langle \eta, \xi^2 \rangle)$ is given. In Table 10 we list the invariant subspaces of \mathcal{N} for squares (2, 2) $((0, 0, w, w)$ with $w \in \mathbf{R}$), stripes (2, 0) $((0, z, 0, 0)$ with $z \in \mathbf{R}$) and squares (2, 0) $((z, w, w, w)$ with $z, w \in \mathbf{R}$). Using these invariant subspaces in NBC and Table 8, it is straightforward to get the eigenvalues of the Jacobian $DF|_{\mathcal{N}}$ along the primary branches of squares (2, 2) and stripes (2, 0) listed in Table 11.

Table 9. Action of $\langle \xi, (0, (1/4)), ((1/4), (1/4)) \rangle$ on $\mathcal{N} \equiv \text{Fix}(\langle \eta, \xi^2 \rangle)$.

ξ	(z_2, z_1, w, w)
$(0, \frac{1}{4})$	$(z_1, -z_2, -w, -w)$
$(\frac{1}{4}, \frac{1}{4})$	$(-z_1, -z_2, w, w)$

Table 10. Invariant subspaces of $\mathcal{N} \equiv \text{Fix}(\langle \eta, \xi^2 \rangle)$ in NBC for squares (2, 2) $((0, 0, w, w)$ with $w \in \mathbf{R}$), stripes (2, 0) $((0, z, 0, 0)$ with $z \in \mathbf{R}$) and squares (2, 0) $((z, z, w, w)$ with $z, w \in \mathbf{R}$).

Isotropy Σ	Invariant subspaces for Σ in NBC	$\ker(\Sigma)$ on V_i^j
$\langle \xi, (\frac{1}{4}, \frac{1}{4}) \rangle$ (squares (2, 2))	$V_1^1 = \mathbf{R}(0, 0, 1, 1)$	$\langle \xi, (\frac{1}{4}, \frac{1}{4}) \rangle$
	$V_2^1 = \mathbf{R}(1, 1, 0, 0)$	ξ
	$V_3^1 = \mathbf{R}(1, -1, 0, 0)$	$\xi(\frac{1}{4}, \frac{1}{4})$
$(\frac{1}{4}, 0)$ (stripes (2, 0))	$V_1^2 = \mathbf{R}(0, 1, 0, 0)$	$(\frac{1}{4}, 0)$
	$V_2^2 = \mathbf{R}\{(0, 0, 1, 1), (1, 0, 0, 0)\}$	1
ξ (squares (2, 0))	$V_1^3 = \mathbf{R}\{(1, 1, 0, 0), (0, 0, 1, 1)\}$	ξ
	$V_2^3 = \mathbf{R}(1, -1, 0, 0)$	1

Note: Note that the kernel $\langle (0, (1/2)), ((1/2), 0) \rangle$ is not recorded in the isotropy subgroups.

The primary branch of squares (2, 0) was discussed in Section 3.3. More information about this branch is needed to understand the possible secondary bifurcations along it.

5.1.1. Squares (2, 0)

We use implicit differentiation for the vector field $F|_{\mathcal{N}}$ given by (5.1) restricted to $\text{Fix}(\mathbf{D}_4)$ to compute the primary branch (z, w, w, w) of squares (2, 0):

$$\begin{aligned}
 w &= -\frac{1}{2A_1} \left[\mu - \lambda + \frac{\alpha}{2A_1A_2} (\mu^2 - \lambda^2) + \frac{\beta}{4A_1^2} (\mu - \lambda)^2 \right] + \dots \\
 z^2 &= \frac{1}{2A_1A_2} (\mu - \lambda)(\mu + \lambda + k_2\lambda^2 + k_3\mu^2 + k_4\lambda\mu) + \dots,
 \end{aligned}
 \tag{5.2}$$

where the values of k_2, k_3 and k_4 can be computed via implicit differentiation of (3.2). We do not compute these values here, but we note that it can be proved using the implicit differentiation that $\mu + \lambda + k_2\lambda^2 + k_3\mu^2 + k_4\lambda\mu + \dots = 0$ implies

$$\mu = -\lambda - \frac{\delta}{A_1^2} \lambda^2 + \dots
 \tag{5.3}$$

The discussion of the eigenvalues of $DF|_{\mathcal{N}}$ along the primary branch (z, w, w, w) of squares (2, 0) is summarized in Table 11 and described in Appendix 2 (see (A12) and (A15)).

Only a Hopf bifurcation can occur along squares (2, 0) in NBC, when the corresponding trace is zero and the corresponding determinant is positive, i.e. $A_1A_2 < 0$

Table 11. Data for secondary bifurcation along squares $S_{2,2}$ $((0, 0, w, w), w > 0$ with $\mu = -\lambda - \delta w^2 + \dots$); stripes $R_{2,0}$ $((0, z, 0, 0)$ with $\mu = \lambda - B_1 z^2 + \dots$); and squares $S_{2,0}$ $((z, z, w, w)$ with $w > 0$ given by (5.2)).

Σ	Eigenvalues (NBC)	Points of secondary bifurcation	Bifurcation occurs when:
$S_{2,2}$	$2\delta w^2 + \dots$	No bifurcation	$\delta \neq 0$
	$\mu - \lambda + 2A_1w + \beta w^2 + \dots$	$\mu_{11} \equiv -\lambda - \frac{\delta}{A_1^2} \lambda^2 + \dots$	$\lambda A_1 > 0$
	$\mu - \lambda - 2A_1w + \beta w^2 + \dots$	$\mu_{12} \equiv -\lambda - \frac{\delta}{A_1^2} \lambda^2 + \dots$	$\lambda A_1 < 0$
$R_{2,0}$	$2B_1z^2 + \dots$	No bifurcation	$B_1 \neq 0$
	tr = $2\mu + (C_1 + \gamma)z^2 + \dots$ det = $-2A_1A_2z^2 + \dots$	$\mu_{22} \equiv \lambda \frac{C_1 + \gamma}{-2B_1 + C_1 + \gamma} + \dots$	$A_1A_2 < 0$ $\lambda(-2B_1 + C_1 + \gamma) < 0$
$S_{2,0}$	$2(\mu - \lambda) + \dots$	No bifurcation	
	tr = $2\mu + 2A_1w + (3\alpha + 2\gamma)z^2 + (\beta + 3\delta)w^2 + \dots$ det = $-4A_1A_2z^2 + \dots$	$\mu_{31} \equiv -\lambda - \frac{3\delta}{A_1^2} \lambda^2 + \dots$	$A_1A_2 < 0$ $\lambda\delta < 0$

Notes: Secondary Hopf bifurcations occur at μ_{22} and μ_{31} ; steady-state bifurcations occur at μ_{11} and μ_{12} .

(see Table 11 and Appendix 2). Substituting the expressions for $S_{2,0}$ solutions given by (5.2) into the trace and using the implicit differentiation for the trace lead to the value of μ_{31} listed in Table 11. The discussion in Section 3.3 and (5.3) show that the primary branch of squares (2, 0) is an isola between $\mu = -\lambda$ and $\mu = -\lambda - (\delta/A_1^2)\lambda^2$ when $A_1A_2 < 0$; in order for Hopf bifurcation to occur at μ_{31} along this isola branch, the point μ_{31} needs to be between $\mu = -\lambda$ and $\mu = -\lambda - (\delta/A_1^2)\lambda^2$. Hence, a simple calculation yields $\lambda\delta < 0$. The expansion of μ_{31} to second order in λ is needed when the stability analysis of squares (2, 0) is discussed.

5.1.2. Non-degeneracy conditions

In the (2, 0) and (2, 2)-mode interaction in the NBC problem, we are interested only in *non-degenerate situations*, i.e. the primary branches have well-defined directions and well-defined stabilities. From Table 6, Section 3.3 and Table 11, we derive the following non-degeneracy conditions in the NBC problem:

$$A_1A_2 \neq 0, \quad B_1 \neq 0, \quad \delta \neq 0.$$

This list shows that there are different possible bifurcation diagrams, which result from the interaction of (2, 0) and (2, 2)-modes in the NBC problem. Moreover, there are other non-degeneracy conditions, which appear when we consider the details of perturbation occurring when $\lambda \neq 0$.

5.2. Squares (2, 0) to squares (2, 2)

To illustrate the continuous transition from squares (2, 0) to squares (2, 2), we determine non-degeneracy conditions for which the region in the $\lambda\mu$ -plane with stable squares (2, 2) is next to the region with stable squares (2, 0). See Figure 5.

Next we discuss the procedure we used to find the non-degeneracy conditions corresponding to Figure 5. Since $(0, 1/4)(z_1, z_2, w, w) = (z_1, -z_2, -w, -w)$, we may assume $w > 0$.

5.2.1. Stripes (2, 0)

Recall that $R_{2,0}$ solutions satisfy $\mu = \lambda - B_1z^2 + \dots$. Hence, $R_{2,0}$ solutions exist in the region of the $\lambda\mu$ -plane given by

$$\frac{\mu - \lambda}{B_1} < 0.$$

Then the non-degeneracy condition $B_1 > 0$ implies that $R_{2,0}$ solutions exist for $\mu - \lambda < 0$ and bifurcates sub-critically at $\mu = \lambda$ for any λ fixed. Table 11 shows that the $R_{2,0}$ branch is unstable, because the eigenvalue $2B_1z^2 + \dots$ is positive.

5.2.2. Squares (2, 2)

Recall that $S_{2,2}$ solutions exist for

$$\frac{\mu + \lambda}{\delta} < 0.$$

$S_{2,2}$ branch is stable if all the eigenvalues of $DF|_{\mathcal{N}}$ along this branch have negative real part. A necessary condition is that the eigenvalue $2\delta w^2 + \dots$ listed in Table 11 is negative. This implies $\delta < 0$, and the region of existence of $S_{2,2}$ solutions in the $\lambda\mu$ -plane is $\lambda + \mu > 0$. A further analysis based on the eigenvalues and points of secondary bifurcations listed in Table 11 shows that $S_{2,2}$ is a stable branch in the region of $\lambda\mu$ -plane given by

$$\mu + \lambda > 0, \quad \mu + \lambda + \frac{\delta}{A_1^2}\lambda^2 < 0 \quad \text{and} \quad \mu(\delta - \beta) + \lambda(\delta + \beta) < 0,$$

where the last inequality is obtained by adding the following eigenvalues of $DF|_{\mathcal{N}}$ along $S_{2,2}$ branch:

$$a_2 = \mu - \lambda + 2A_1w + \beta w^2 + \dots$$

and

$$a_3 = \mu - \lambda - 2A_1w + \beta w^2 + \dots,$$

after substituting $w^2 = -(\lambda + \mu/\delta) + \dots$.

The line $\mu(\delta - \beta) + \lambda(\delta + \beta) = 0$ divides the $\lambda\mu$ -plane in two regions. See line 3 in Figure 5. The signs of $\delta + \beta$ and $\delta - \beta$ determine which region (left or right) between the line $\mu + \lambda = 0$ and the parabola $\mu + \lambda + (\delta/A_1^2)\lambda^2 = 0$ contains stable $S_{2,2}$ solutions. To get the correct region, we need $\delta + \beta < 0$ and $\delta - \beta < 0$, which implies that the inequality $\delta < 0$ is redundant.

5.2.3. Squares (2, 0)

Recall that the isola of squares (2, 0) as μ varies exists between λ and $-\lambda - (\delta/A_1^2)\lambda^2$ when $A_1A_2 < 0$. $S_{2,0}$ solutions branch is stable if all the eigenvalues of $DF|_{\mathcal{N}}$ along it have negative real part. A further analysis based on Table 11 gives the region of stability for the isola of $S_{2,0}$ solutions in the $\lambda\mu$ -plane:

$$\mu - \lambda < 0, \quad \mu + \lambda + \frac{\delta}{A_1^2}\lambda^2 > 0 \quad \text{and} \quad \mu + \lambda + \frac{3\delta}{A_1^2}\lambda^2 > 0.$$

Since $\delta < 0$, we have an open region of stable $S_{2,0}$ solutions in the $\lambda\mu$ -plane. Curves 1 and 2 in Figure 5 have equations $\mu + \lambda + (\delta/A_1^2)\lambda^2 = 0$ and $\mu + \lambda + (3\delta/A_1^2)\lambda^2 = 0$, respectively.

Along the isola of $S_{2,0}$ solutions we have $w = -(1/2A_1)(\mu - \lambda) + \dots > 0$ and $\mu - \lambda < 0$. It follows that $A_1 > 0$, which combined with $A_1A_2 < 0$ yields $A_2 < 0$.

5.2.4. Non-degeneracy conditions

Previous analysis gives the following open set of non-degeneracy conditions:

$$A_1 > 0, \quad A_2 < 0, \quad B_1 > 0, \quad \delta - \beta < 0 \quad \text{and} \quad \delta + \beta < 0. \tag{5.4}$$

5.3. Squares (2, 2) to stripes (2, 0)

In order to determine possible transitions from squares (2, 2) to stripes (2, 0), we trace paths through unfoldings of the (2, 0) and (2, 2)-mode interaction and we determine non-degeneracy conditions for which the following two types of transitions are observed in the $\lambda\mu$ -plane:

- (a) transition from squares (2, 2) to squares (2, 0) and, then to stripes (2, 0) via some other stable states – one possible situation being via time-periodic solutions (standing waves). See Figure 6 (left);
- (b) transition from squares (2, 2) to stripes (2, 0) via jump. See Figure 6 (right).

In what follows we discuss the procedure to get the non-degeneracy conditions corresponding to Figure 6. As before, since $(0, 1/4)(z_1, z_2, w, w) = (z_1, -z_2, -w, -w)$, we may assume $w > 0$.

For both cases (a) and (b), we retain the non-degeneracy conditions obtained in Section 5.2 for stable squares (2, 0). For case (a), we also use the non-degeneracy conditions obtained in Section 5.2 for stable squares (2, 2). In this section, we determine non-degeneracy conditions such that an open region of stable stripes $R_{2,0}$ exists in the $\lambda\mu$ -plane for both cases (a) and (b). Also, we determine non-degeneracy conditions for stable squares (2, 2) in case (b). Note that the equations for curves 1 and 2 in Figure 6 are $\mu + \lambda + (\delta/A_1^2)\lambda^2 = 0$ and $\mu + \lambda + (3\delta/A_1^2)\lambda^2 = 0$, respectively; and that the equation for line 3 is $\mu(\delta - \beta) + \lambda(\delta + \beta) = 0$.

5.3.1. Stripes (2, 0)

Recall that $R_{2,0}$ solutions exist for $(\mu - \lambda/B_1) < 0$. The $R_{2,0}$ branch is stable if all the eigenvalues of $DF|_{\mathcal{N}}$ along this branch have negative real part. A necessary condition is that the eigenvalue $2B_1z^2 + \dots$ listed in Table 11 is negative. Hence, $B_1 < 0$ and the region of existence of stripes (2, 0) in the $\lambda\mu$ -plane is $\mu - \lambda > 0$. A further analysis based on Table 11 gives the region of stability for $R_{2,0}$ branch in the $\lambda\mu$ -plane:

$$\mu - \lambda > 0 \quad \text{and} \quad \mu(2B_1 - C_1 - \gamma) + \lambda(C_1 + \gamma) > 0.$$

The line $\mu(2B_1 - C_1 - \gamma) + \lambda(C_1 + \gamma) = 0$ divides the $\lambda\mu$ -plane in two regions. (See curve 4 in Figure 6). The signs of $2B_1 - C_1 - \gamma$ and $C_1 + \gamma$ determine the quadrants ((I and III) or (II and IV)) in which the line $\mu(2B_1 - C_1 - \gamma) + \lambda(C_1 + \gamma) = 0$ is contained, and which region (left or right) between the lines $\mu - \lambda = 0$ and $\mu(2B_1 - C_1 - \gamma) + \lambda(C_1 + \gamma) = 0$ contains stable $R_{2,0}$ solutions.

To get the left region of stable stripes (2, 0), as in Figure 6 (left), it is enough to choose $C_1 + \gamma < 0$ and $2B_1 - C_1 - \gamma > 0$. Since $B_1 < 0$, the inequality $C_1 + \gamma < 0$ is redundant.

5.3.2. Non-degeneracy conditions for (a)

Previous analysis gives the following open set of non-degeneracy conditions for Figure 6 (left):

$$\begin{aligned} A_1 > 0, \quad A_2 < 0, \quad \delta - \beta < 0, \quad \delta + \beta < 0, \\ B_1 < 0 \quad \text{and} \quad 2B_1 - C_1 - \gamma > 0. \end{aligned} \tag{5.5}$$

5.3.3. *Non-degeneracy conditions for (b)*

Similarly, the open set of non-degeneracy conditions for Figure 6 (right) is:

$$\begin{aligned} A_1 > 0, \quad A_2 < 0, \quad \delta < 0, \quad \delta - \beta > 0, \\ -B_1 + C_1 + \gamma < 0 \quad \text{and} \quad 2B_1 - C_1 - \gamma < 0. \end{aligned} \tag{5.6}$$

Namely, to get the left region of squares (2, 2), as in Figure 6 (right), is enough to choose $\delta + \beta < 0$ and $\delta - \beta > 0$. Since $\delta < 0$, the inequality $\delta + \beta < 0$ is redundant.

To get a non-empty overlapping region of stable $R_{2,0}$ solutions and stable $S_{2,2}$ solutions, as in Figure 6 (right), we need

$$2B_1 - C_1 - \gamma < 0 \quad \text{and} \quad C_1 + \gamma < 0$$

(the line $\mu(2B_1 - C_1 - \gamma) + \lambda(C_1 + \gamma) = 0$ is contained in quadrants (II and IV) and the stable $R_{2,0}$ solutions are to the left of this line) and the slope of the line $\mu(2B_1 - C_1 - \gamma) + \lambda(C_1 + \gamma) = 0$ needs to satisfy the inequality

$$-\frac{C_1 + \gamma}{2B_1 - C_1 - \gamma} < -1.$$

All these imply the inequality $-B_1 + C_1 + \gamma < 0$. Also, $-B_1 + C_1 + \gamma < 0$ and $2B_1 - C_1 - \gamma < 0$ imply that the inequalities $B_1 < 0$ and $C_1 + \gamma < 0$ are redundant.

The thick lines parameterized by μ for fixed λ , as in Figures 6, lead to the bifurcation diagrams in Figure 7. In these figures, the primary branch of squares (2, 2) bifurcates at $\mu = -\lambda$ from the trivial solution and is stable until $\mu = \mu_{11}$, where a stable isola of squares (2, 0) bifurcates. This isola branch loses stability at $\mu = \mu_{31}$ via a sub-critical or supercritical Hopf bifurcation leading to time-periodic solutions (standing waves).

The primary branch of stripes (2, 0) bifurcates at $\mu = \lambda$ from the trivial solution and is unstable till $\mu = \mu_{31}$, where a sub-critical Hopf bifurcation occurs leading to stable time-periodic solutions (standing waves) in NBC.

The tertiary branch of time-periodic solutions bifurcating from $\mu = \mu_{31}$ may connect to the secondary branch of time-periodic solutions bifurcating from $\mu = \mu_{22}$. As a consequence, the transition from squares (2, 2) to stripes (2, 0) occurs via squares (2, 0) and standing waves.

5.4. Differences between NBC and PBC problems

In this section we discuss interesting differences related to different stable patterns observed in the NBC and PBC problems. To simplify the discussion, we restrict the $\mathbf{D}_4 \times \mathbf{T}^2$ -equivariant vector field F to the flow-invariant subspace

$$\text{Fix}(\xi^2) = \{(z_1, z_2, w_1, w_2) : z_1, z_2, w_1, w_2 \in \mathbf{R}\} = \mathbf{R}^4.$$

As a consequence, the primary branch of stripes (2, 2) ($R_{2,2}$ branch) exists. Throughout this subsection, we impose non-degeneracy conditions such that this branch is unstable.

The $\mathbf{D}_4 \times \mathbf{T}^2$ -equivariant vector field F truncated up to the third-order and restricted to $\text{Fix}(\langle \xi^2 \rangle) = \mathbf{R}^4$ is given by

$$\begin{aligned}
 f^1(z_1, z_2, w_1, w_2, \lambda, \mu) &= (-\lambda + \mu)z_1 + A_1 z_2(w_1 + w_2) + E_1 z_1 w_1 w_2 \\
 &\quad + [B_1 z_1^2 + C_1 z_2^2 + D_1(w_1^2 + w_2^2)]z_1 \\
 f^2(z_1, z_2, w_1, w_2, \lambda, \mu) &= (-\lambda + \mu)z_2 + A_1 z_1(w_1 + w_2) + E_1 z_2 w_1 w_2 \\
 &\quad + [B_1 z_2^2 + C_1 z_1^2 + D_1(w_1^2 + w_2^2)]z_2 \\
 g^1(z_1, z_2, w_1, w_2, \lambda, \mu) &= (\lambda + \mu)w_1 + A_2 z_1 z_2 + E_2(z_1^2 + z_2^2)w_2 \\
 &\quad + [B_2(z_1^2 + z_2^2) + C_2 w_1^2 + D_2 w_2^2]w_1 \\
 g^2(z_1, z_2, w_1, w_2, \lambda, \mu) &= (\lambda + \mu)w_2 + A_2 z_1 z_2 + E_2(z_1^2 + z_2^2)w_1 \\
 &\quad + [B_2(z_1^2 + z_2^2) + C_2 w_2^2 + D_2 w_1^2]w_2,
 \end{aligned} \tag{5.7}$$

where $F|_{\mathbf{R}^4} = (f^1, f^2, g^1, g^2): \mathbf{R}^4 \times \mathbf{R}^2 \rightarrow \mathbf{R}^4$. Recall that we have defined the following constants:

$$\alpha = B_1 + C_1, \quad \beta = 2D_1 + E_1, \quad \gamma = B_2 + E_2 \quad \text{and} \quad \delta = C_2 + D_2.$$

Table 8 shows that along the $R_{2,0}$ branch a new steady state bifurcation can occur in $\text{Fix}(\langle \xi^2 \rangle)$ at μ_{21} . This leads to the following *generic* situation: in the NBC problem we see time-periodic solutions (*standing waves*) as stable patterns leading to stable stripes $(2, 0)$, whereas in the PBC problem we see steady states (*wavy rolls*) as stable patterns leading to stable stripes $(2, 0)$.

We can follow the same approach as for the restriction to the NBC problem: determine regions of various stable steady states (Figure 8) and trace a path in the $\lambda\mu$ -plane to illustrate different transitions from squares $(2, 2)$ to stripes $(2, 0)$ in the NBC and PBC problems: transition via a steady state bifurcation in the PBC problem (Figure 8) and transition via a Hopf bifurcation in the NBC problem (Figure 6).

5.4.1. Wavy rolls solutions

Implicit differentiation for the truncated normal form given in (5.7) leads to a new branch of steady states $(0, z, w, -w)$ of small amplitudes – called *wavy rolls*:

$$\begin{aligned}
 z^2 &= \frac{(-2D_1 + E_1 - \delta)\mu + (-2D_1 + E_1 + \delta)\lambda}{K_s} + \dots \\
 w^2 &= \frac{(B_1 - B_2 + E_2)\mu + (B_1 + B_2 - E_2)\lambda}{K_s} + \dots,
 \end{aligned} \tag{5.8}$$

where $K_s = B_1\delta - (2D_1 - E_1)(E_2 - B_2)$. The region of existence for *wavy rolls* solutions in the $\lambda\mu$ -plane is:

$$\begin{aligned}
 \frac{(-2D_1 + E_1 - \delta)\mu + (-2D_1 + E_1 + \delta)\lambda}{K_s} &\geq 0 \\
 \frac{(B_1 - B_2 + E_2)\mu + (B_1 + B_2 - E_2)\lambda}{K_s} &\geq 0.
 \end{aligned}$$

5.4.2. *Stripes (2, 2)*

Recall that $R_{2,2}$ solutions have the form $(0, 0, 0, w)$ with $\mu = -\lambda - C_2 w^2 + \dots$ and they exist in the PBC problem in the region of the $\lambda\mu$ -plane given by

$$\frac{\mu + \lambda}{C_2} < 0.$$

The eigenvalues of the Jacobian of the restriction of the vector field F to $\text{Fix}(\langle \xi^2 \rangle)$ along squares $(2, 2)$, squares $(2, 0)$, stripes $(2, 2)$ and wavy rolls $(0, z, w, -w)$ help us to determine the stability of these solution branches. The information about these eigenvalues is summarized in Tables 12 and 13. The calculations needed to obtain these tables can be found in Appendix 2. Table 12 contains the eigenvalues of the Jacobian of the vector field $F|_{\text{Fix}(\langle \xi^2 \rangle)}$ along squares $(2, 2)$ and stripes $(2, 0)$, which is straightforward to obtain from Table 8.

A possible generic situation showing regions of the various stable steady states mentioned before in this section is presented in Figure 8. The corresponding set of non-degeneracy conditions can be determined, but we do not pursue this matter

Table 12. Data for secondary bifurcations in $\text{Fix}(\langle \xi^2 \rangle)$ along squares $S_{2,2}$ $((0, 0, w, w), w) 0$ with $\mu = -\lambda - (C_2 + D_2)w^2 + \dots$; stripes $R_{2,0}$ $((0, z, 0, 0)$ with $\mu = \lambda - B_1 z^2 + \dots$); and squares $S_{2,0}$ $((z, z, w, w)$ with $w > 0$ defined by (5.2)).

Σ	Eigenvalues ($\text{Fix}(\langle \xi^2 \rangle)$)	Points of secondary bifurcation	Bifurcation occurs when:
$S_{2,2}$	$2\delta w^2 + \dots$	No bifurcation	$\delta \neq 0$
	$\mu - \lambda + 2A_1 w + \beta w^2 + \dots$	$\mu_{11} \equiv -\lambda - \frac{\delta}{A_1^2} \lambda^2 + \dots$	$\lambda A_1 > 0$
	$\mu - \lambda - 2A_1 w + \beta w^2 + \dots$	$\mu_{12} \equiv -\lambda - \frac{\delta}{A_1^2} \lambda^2 + \dots$	$\lambda A_1 < 0$
	$2(C_2 - D_2)w^2 + \dots$	No bifurcation	$C_2 \neq D_2$
$R_{2,0}$	$2B_1 z^2 + \dots$	No bifurcation	$B_1 \neq 0$
	$\mu + \lambda + (B_2 - E_2)z^2 + \dots$	$\mu_{21} \equiv \lambda \frac{-B_1 - B_2 + E_2}{B_1 - B_2 + E_2} + \dots$	$\lambda(B_1 - B_2 + E_2) > 0$
	$\text{tr} = 2\mu + (C_1 + \gamma)z^2 + \dots$ $\text{det} = -2A_1 A_2 z^2 + \dots$	$\mu_{22} \equiv \lambda \frac{C_1 + \gamma}{-2B_1 + C_1 + \gamma} + \dots$	$A_1 A_2 < 0$ $\lambda(-2B_1 + C_1 + \gamma) < 0$
$S_{2,0}$	$2(\mu - \lambda) + \dots$	No bifurcation	
	$\text{tr} = 2\mu + 2A_1 w + (3\alpha + 2\gamma)z^2$ $+ (\beta + 3\delta)w^2 + \dots$	$\mu_{31} \equiv -\lambda - \frac{3\delta}{A_1^2} \lambda^2 + \dots$	$A_1 A_2 < 0$ $\lambda \delta < 0$
	$\text{det} = -4A_1 A_2 z^2 + \dots$		
	$\mu + \lambda + 2B_2 z^2 + (3C_2 - D_2)w^2$ $+ \dots$	$\mu_{32} = -\lambda - \frac{3C_2 - D_2}{2A_1^2} \lambda^2$ $+ \dots$	$\lambda(C_2 - D_2) < 0$

Notes: Secondary Hopf bifurcations occur at μ_{22} and μ_{31} ; the remaining bifurcations are steady state.

Table 13. Data for (steady-state) secondary bifurcations in $\text{Fix}(\langle \xi^2 \rangle)$ along stripes $R_{2,2}$ $((0, 0, 0, w), w > 0$ with $\mu = -\lambda - C_2 w^2 + \dots$) and wavy rolls WR $((0, z, w, -w)$ with $w > 0$.

Σ	Eigenvalues ($\text{Fix}(\langle \xi^2 \rangle)$)	Points of secondary bifurcation	Bifurcations occur when:
$R_{2,2}$	$\mu - \lambda - A_1 w + D_1 w^2 + \dots$	$\mu_{41} = -\lambda - \frac{2C_2}{A_1^2} \lambda^2 + \dots$	$\lambda A_1 > 0$
	$\mu - \lambda + A_1 w + D_1 w^2 + \dots$	$\mu_{42} = -\lambda - \frac{2C_2}{A_1^2} \lambda^2 + \dots$	$\lambda A_1 < 0$
	$2C_2 w^2 + \dots + \dots$	No bifurcation	$C_2 \neq 0$
$(0, z, w, -w)$	$(D_2 - C_2)w^2 + \dots$	No bifurcation	$C_2 \neq D_2$
	$4\delta w^2 + \dots$	No bifurcation	$\delta \neq 0$
<i>(wavy rolls)</i>	$\begin{pmatrix} U_1 & 0 & Z_1 \\ 0 & U_2 & Z_2 \\ 2V & 2V & Q \end{pmatrix}$	*	

Note: w and z are defined by (5.8); U_1, U_2, V, Z_1, Z_2 and Q are defined by (5.9).
 *Indicates that other bifurcations might occur.

here – since it is difficult to find the eigenvalues of the 3×3 matrix

$$\begin{pmatrix} U_1 & 0 & Z_1 \\ 0 & U_2 & Z_2 \\ 2V & 2V & Q \end{pmatrix}.$$

where

$$\begin{aligned} Q &= 2(E_2 z^2 + 2C_2 w^2) + \dots \\ U_1 &= 2B_1 z^2 + \dots \\ U_2 &= (C_1 - B_1)z^2 + \dots \\ V &= A_1 z + \dots \\ Z_1 &= A_2 z + \dots \\ Z_2 &= 2(B_2 + E_2)zw + \dots \end{aligned} \tag{5.9}$$

The expressions for Q, V, U_1, U_2, Z_1 and Z_2 are computed in Appendix 2.

We trace a thick line path parameterized by μ for $\lambda > 0$ fixed in Figure 8 to show the transition from stable squares $(2, 2)$ to stable stripes $(2, 0)$ via stable squares $(2, 0)$ and stable wavy rolls steady states $(0, z, w, -w)$.

Acknowledgements

The research of AC was supported in part by an NSERC Postgraduate Fellowship. The research was supported in part by NSF Grants DMS-0244529 and DMS-0604429. The authors would like to thank the Isaac Newton Institute for its hospitality and support.

References

- [1] A.M. Turing, *The chemical basis of morphogenesis*, Phil. Trans. Roy. Soc. Lond. B 237 (1952), pp. 37–72.
- [2] V. Castets et al., *Experimental evidence of a sustained Turing-type equilibrium chemical pattern*, Phys. Rev. Lett. 64(3) (1990), pp. 2953–2956.
- [3] Q. Ouyang and H.L. Swinney, *Transition from a uniform state to hexagonal and striped Turing patterns*, Nature 352 (1991), pp. 610–612.
- [4] S. Srinivasan, K.E. Rashka, and E. Bier, *Creation of a Sog morphogen gradient in the Drosophila embryo*, Dev. Cell 2 (2002), pp. 91–101.
- [5] M. Baringa, *Looking to development's future*, Science 266 (1994), pp. 561–564.
- [6] E.J. Crampin, E.A. Gaffney, and P.K. Maini, *Reaction and diffusion on growing domains: Scenarios for robust pattern formation*, Bull. Math. Biol. 61(6) (1999), pp. 1093–1120.
- [7] E.J. Crampin, *Reaction-diffusion Patterns on Growing Domains*, PhD Thesis, Magdalen College, University of Oxford, 2000.
- [8] R. Plaza et al., *The effect of growth and curvature on pattern formation*, J. Dynam. Diff. Eqns. 16(4) (2004), pp. 1093–1121.
- [9] S. Kondo and R. Asai, *A reaction-diffusion wave on the skin of the marine angelfish Pomacanthus*, Nature 376 (1995), pp. 765–768.
- [10] E.J. Crampin, E.A. Gaffney, and P.K. Maini, *Mode doubling and tripling in reaction-diffusion patterns on growing domains: A piecewise linear model*, J. Math. Biol. 44(2) (2002), pp. 107–128.
- [11] A. Madzvamuse, A.J. Wathen, and P.K. Maini, *A moving grid finite element method applied to a model biological pattern generator*, J. Comp. Phys. 190 (2003), pp. 478–500.
- [12] —, *A moving grid finite element method for the simulation of pattern generation by Turing models on growing domains*, J. Sci. Comput. 24(2) (2005), pp. 247–262.
- [13] E. Izhikevich, *Neural excitability, spiking and bursting*, Int. J. Bif. Chaos 10(6) (2000), pp. 1171–1266.
- [14] M. Golubitsky, K. Josic, and T.J. Kaper, *An unfolding theory approach to bursting in fast-slow systems*, in *Global Analysis of Dynamical Systems: Festschrift dedicated to Floris Takens on the occasion of his 60th birthday*, H.W. Broer, B. Krauskopf, and G. Vegter, eds., Institute of Physics Publ, Bristol, 2001, pp. 277–308.
- [15] J.D. Crawford et al., *Boundary conditions as symmetry constraints*, in *Singularity Theory and Its Applications, Warwick 1989, Part II.*, Vol. 1463, Lecture Notes in Math, M. Roberts and I.N. Stewart, eds., Springer-Verlag, Heidelberg, 1991, pp. 63–79.
- [16] J.D. Crawford, *Surface waves in non-square containers with square symmetry*, Phys. Rev. Lett. 67 (1991), pp. 441–444.
- [17] M. Golubitsky and I. Stewart, *The Symmetry Perspective*, Vol. 200, Progress in Mathematics, Birkhäuser, Basel, 2002.
- [18] J.D. Crawford, J.P. Gollub, and D. Lane, *Hidden symmetries of parametrically forced waves*, Nonlinearity 6 (1993), pp. 119–164.
- [19] M. Golubitsky, I.N. Stewart, and D.G. Schaeffer, *Singularities and Groups in Bifurcation Theory*: Vol. 69, Applied Mathematical Sciences, Springer-Verlag, New York, 1988.
- [20] J.D. Crawford, *D_4 -symmetric Maps with hidden Euclidean symmetry*, in *Pattern Formation and Symmetry Breaking in PDE's*, Vol. 5, J. Chadan, M. Golubitsky, W. Langford, and B. Wetton, eds., Fields Institute Communications, AMS, Providence, 1996.
- [21] J.W. Swift, *Bifurcation and Symmetry in Convection*, PhD Thesis, University of California, Berkeley, 1984.
- [22] M.R.E. Proctor and P.C. Matthews, *$\sqrt{2} : 1$ Resonance in non-Boussinesq convection*, Physica D 97 (1996), pp. 229–241.

[23] M. Golubitsky, I.N. Stewart, and D.G. Schaeffer, *Singularities and Groups in Bifurcation Theory*, Vol. 51, Applied Mathematical Sciences, Springer-Verlag, New York, 1984.

Appendix 1. Third-Order truncation of F

In this appendix we re-derive the normal form of the $\mathbf{D}_4 \times \mathbf{T}^2$ -equivariant vector field F truncated up to third-order terms (given in (3.1)). We recall that the action of $\mathbf{D}_4 \times \mathbf{T}^2$ is given in Table 1 and $\mathbf{D}_4 = \langle \eta, \xi \rangle$.

Let $F = (f^1, f^2, g^1, g^2) : \mathbf{C}^2 \times \mathbf{C}^2 \rightarrow \mathbf{C}^2 \times \mathbf{C}^2$ be $\mathbf{D}_4 \times \mathbf{T}^2$ -equivariant. The $\eta\xi^3$ -equivariance and $\eta\xi^2$ -equivariance of F imply

$$\begin{aligned} f^2(z_1, z_2, w_1, w_2) &= f^1(z_2, z_1, w_1, \overline{w_2}) \\ g^2(z_1, z_2, w_1, w_2) &= g^1(z_1, \overline{z_2}, w_2, w_1). \end{aligned}$$

Therefore, it is sufficient to find the forms of f^1 and g^1 up to third-order. Let

$$\begin{aligned} f^1(z_1, z_2, w_1, w_2) &= \sum a_{\alpha_1 \beta_1 \gamma_1 \delta_1 \alpha_2 \beta_2 \gamma_2 \delta_2} z_1^{\alpha_1} \overline{z_1}^{\alpha_2} z_2^{\beta_1} \overline{z_2}^{\beta_2} w_1^{\gamma_1} \overline{w_1}^{\gamma_2} w_2^{\delta_1} \overline{w_2}^{\delta_2} \\ g^1(z_1, z_2, w_1, w_2) &= \sum b_{\alpha_1 \beta_1 \gamma_1 \delta_1 \alpha_2 \beta_2 \gamma_2 \delta_2} z_1^{\alpha_1} \overline{z_1}^{\alpha_2} z_2^{\beta_1} \overline{z_2}^{\beta_2} w_1^{\gamma_1} \overline{w_1}^{\gamma_2} w_2^{\delta_1} \overline{w_2}^{\delta_2}, \end{aligned} \tag{A1}$$

where $\alpha_i, \beta_i, \gamma_i, \delta_i$ are non-negative integers and the subscripted constants a, b are complex. Note, however, that ξ^2 -equivariance forces these constants to be real.

Truncated form of f^1 up to third-order terms

\mathbf{T}^2 -equivariance of F implies

$$\begin{aligned} \alpha_1 - \alpha_2 + \gamma_1 - \gamma_2 + \delta_1 - \delta_2 &= 1 \\ \beta_1 - \beta_2 + \gamma_1 - \gamma_2 - \delta_1 + \delta_2 &= 0 \end{aligned} \tag{A2}$$

and third-order truncation implies

$$\alpha_1 + \alpha_2 + \beta_1 + \beta_2 + \gamma_1 + \gamma_2 + \delta_1 + \delta_2 \leq 3.$$

Therefore, if we consider all possible cases in (A2), we get

$$\begin{aligned} f^1(z_1, z_2, w_1, w_2) &= a_1 z_1 + b_1 z_2 w_2 + c_1 \overline{z_2} w_1 + E_1 \overline{z_1} w_1 w_2 \\ &\quad + B_1 |z_1|^2 z_1 + C_1 |z_2|^2 z_1 + d_1 |w_1|^2 z_1 + e_1 |w_2|^2 z_1, \end{aligned} \tag{A3}$$

where $a_1, b_1, c_1, d_1, e_1, B_1, C_1, E_1$ are real. The η -equivariance of F implies that $b_1 = c_1 \equiv A_1$ and $d_1 = e_1 \equiv D_1$.

Truncated form of g^1 up to third-order terms

The \mathbf{T}^2 -equivariance of F implies

$$\begin{aligned} \alpha_1 - \alpha_2 + \gamma_1 - \gamma_2 + \delta_1 - \delta_2 &= 1 \\ \beta_1 - \beta_2 + \gamma_1 - \gamma_2 - \delta_1 + \delta_2 &= 1. \end{aligned} \tag{A4}$$

and third-order truncation implies

$$\alpha_1 + \alpha_2 + \beta_1 + \beta_2 + \gamma_1 + \gamma_2 + \delta_1 + \delta_2 \leq 3.$$

Therefore, if we consider all possible cases in (A.4), we get

$$g^1(z_1, z_2, w_1, w_2) = a_2 w_1 + A_2 z_1 z_2 + b_2 z_1^2 \bar{w}_2 + c_2 z_2^2 w_2 + d_2 |z_1|^2 w_1 + e_2 |z_2|^2 w_1 + C_2 |w_1|^2 w_1 + D_2 |w_2|^2 w_1 \tag{A5}$$

where $a_2, b_2, c_2, d_2, e_2, C_2, D_2, E_2$ are real. The η -equivariance of F implies that $d_2 = e_2 \equiv B_2$ and $b_2 = c_2 \equiv E_2$.

Appendix 2. Eigenvalues of DF along primary branches

In this appendix we compute the eigenvalues listed in Tables 8, 12 and 13. To simplify the notation, we omit explicit reference to the parameters λ and μ in F . As before, $F: \mathbb{C}^4 \rightarrow \mathbb{C}^4$ is a function of the complex variables $z_1, \bar{z}_1, z_2, \bar{z}_2, w_1, \bar{w}_1, w_2, \bar{w}_2$. In these coordinates the Jacobian $(DF)_{(z_1, z_2, w_1, w_2)}$ can be written as

$$(DF)_{(z_1, z_2, w_1, w_2)}(u_1, u_2, v_1, v_2) = F_{z_1} u_1 + F_{\bar{z}_1} \bar{u}_1 + F_{z_2} u_2 + F_{\bar{z}_2} \bar{u}_2 + F_{w_1} v_1 + F_{\bar{w}_1} \bar{v}_1 + F_{w_2} v_2 + F_{\bar{w}_2} \bar{v}_2. \tag{A6}$$

Eigenvalues of DF along squares (2, 2) (Table 8)

Let $V_j^1 (1 \leq j \leq 6)$ be the isotypic components listed in Table 7. Recall that $S_{2,2}$ solutions have the form $(0, 0, w, w)$ where $w \in \mathbb{R}$ and

$$(DF)_{(0,0,w,w)}(V_j^1) \subset V_j^1.$$

Recall also that V_1^1, \dots, V_4^1 are one dimensional, V_5^1 is a two-dimensional null space of $(DF)_{(0,0,w,w)}$, and V_6^1 is a two-dimensional absolutely irreducible representation of $S_{2,2}$. Hence, in a basis adapted to the subspaces V_1^j , we get the block diagonalization

$$(DF)_{(0,0,w,w)} = \begin{pmatrix} a_1 & 0 & 0 & 0 & 0 & 0 \\ 0 & a_2 & 0 & 0 & 0 & 0 \\ 0 & 0 & a_3 & 0 & 0 & 0 \\ 0 & 0 & 0 & a_4 & 0 & 0 \\ 0 & 0 & 0 & 0 & 0 & 0 \\ 0 & 0 & 0 & 0 & 0 & a_6 I \end{pmatrix},$$

where $a_i \in \mathbb{R}$. It follows that any vector in V_1^j is an eigenvector of $(DF)_{(0,0,w,w)}$ and these vectors are listed in Table 7. Thus

$$\begin{aligned} (DF)_{(0,0,w,w)}(0, 0, 1, 1) &= F_{w_1} + F_{\bar{w}_2} + F_{w_2} + F_{\bar{w}_1} \\ &= (g_{w_1}^1 + g_{\bar{w}_1}^3 + g_{w_2}^1 + g_{\bar{w}_2}^1)(0, 0, 1, 1); \\ (DF)_{(0,0,w,w)}(1, 1, 0, 0) &= F_{z_1} + F_{\bar{z}_1} + F_{z_2} + F_{\bar{z}_2} \\ &= (f_{z_1}^1 + f_{\bar{z}_1}^1 + f_{z_2}^1 + f_{\bar{z}_2}^1)(1, 1, 0, 0); \\ (DF)_{(0,0,w,w)}(1, -1, 0, 0) &= F_{z_1} + F_{\bar{z}_1} - F_{z_2} - F_{\bar{z}_2} \\ &= (f_{z_1}^1 + f_{\bar{z}_1}^1 - f_{z_2}^1 - f_{\bar{z}_2}^1)(1, -1, 0, 0); \\ (DF)_{(0,0,w,w)}(0, 0, 1, -1) &= F_{w_1} + F_{\bar{w}_1} - F_{w_2} - F_{\bar{w}_2} \\ &= (g_{w_1}^1 + g_{\bar{w}_1}^1 - g_{w_2}^1 - g_{\bar{w}_2}^1)(0, 0, 1, -1); \\ (DF)_{(0,0,w,w)}(i, 0, 0, 0) &= F_{z_1} i - F_{\bar{z}_1} i + F_{z_2} i - F_{\bar{z}_1} i \\ &= (f_{z_1}^1 - f_{\bar{z}_1}^1)(i, 0, 0, 0). \end{aligned}$$

where the partial derivatives are evaluated at $(0, 0, w, w)$. Here we used the facts $f_{z_1}^2 = f_{z_1}^1$ and $f_{z_1}^2 = f_{z_1}^1$ along $(0, 0, w, w)$.

Using the third-order truncation of the $\mathbf{D}_4 \times \mathbf{T}^2$ -equivariant vector field F given in (3.1), it follows that

$$\begin{aligned}
 a_1 &= g_{w_1}^1 + g_{\overline{w_1}}^1 + g_{w_2}^1 + g_{\overline{w_2}}^1 &= \lambda + \mu + 3\delta w^2 + \dots \\
 a_2 &= f_{z_1}^1 + f_{\overline{z_1}}^1 + f_{z_2}^1 + f_{\overline{z_2}}^1 &= -\lambda + \mu + 2A_1 w + \beta w^2 + \dots \\
 a_3 &= f_{z_1}^1 + f_{\overline{z_1}}^1 - f_{z_2}^1 - f_{\overline{z_2}}^1 &= -\lambda + \mu - 2A_1 w + \beta w^2 + \dots \\
 a_4 &= g_{w_1}^1 + g_{\overline{w_1}}^1 - g_{w_2}^1 - g_{\overline{w_2}}^1 &= \lambda + \mu + (3C_2 - D_2)w^2 + \dots \\
 a_6 &= f_{z_1}^1 - f_{\overline{z_1}}^1 &= -\lambda + \mu + (2D_1 - E_1)w^2 + \dots
 \end{aligned} \tag{A7}$$

Along squares (2, 2) we have $\mu = -\lambda - \delta w^2 + \dots$. The eigenvalues listed in Table 8 for the isotropy subgroup $S_{2,2}$ are found by substituting this equation into (A7).

Eigenvalues of DF along stripes (2, 0) (Table 8)

Let $V_j^2 (1 \leq j \leq 4)$ be the isotypic components defined in Table 7, where V_1^2 and V_2^2 are one-dimensional, V_3^2 is the null eigenspace of $(DF)_{(0,z,0,0)}$, V_3^2 is a two-dimensional irreducible representation and V_4^2 consists of two isomorphic two-dimensional absolutely irreducible subspaces. Recall that $R_{2,0}$ solutions have the form $(0, z, 0, 0)$ where $z \in \mathbf{R}$ and that

$$(DF)_{(0,z,0,0)}(V_j^2) \subset V_j^2$$

for $j = 1, \dots, 4$. Hence, we get the block diagonalization

$$(DF)_{(0,z,0,0)} = \begin{pmatrix} b_1 & 0 & 0 & 0 & 0 \\ 0 & 0 & 0 & 0 & 0 \\ 0 & 0 & b_3 I & 0 & 0 \\ 0 & 0 & 0 & b_4 I & b_5 I \\ 0 & 0 & 0 & b_6 I & b_7 I \end{pmatrix},$$

where $b_i \in \mathbf{R}$. It follows that the seven non-zero eigenvalues of DF are b_1, b_3 repeated twice, and the eigenvalues of $\begin{pmatrix} b_4 & b_5 \\ b_6 & b_7 \end{pmatrix}$ repeated twice. Table 7 along $(0, 0, z, 0)$ gives

$$\begin{aligned}
 (DF)_{(0,z,0,0)}(0, 1, 0, 0) &= F_{z_2} + F_{z_2} &= (f_{z_2}^2 + f_{z_2}^2)(0, 1, 0, 0); \\
 (DF)_{(0,z,0,0)}(0, 0, 1, -1) &= F_{w_1} + F_{\overline{w_1}} - F_{w_2} - F_{\overline{w_2}} &= (g_{w_1}^1 + g_{\overline{w_1}}^1 - g_{w_2}^1 - g_{\overline{w_2}}^1)(0, 0, 1, -1)
 \end{aligned}$$

The four-dimensional subspace V_4^2 consists of vectors of the form $(u, 0, v, w)$ where $u, v \in \mathbf{C}$. To compute b_4, \dots, b_7 we need only compute

$$\begin{aligned}
 (DF)_{(0,z,0,0)}(1, 0, 0, 0) &= b_4(1, 0, 0, 0) + b_6(0, 0, 1, 1) \\
 (DF)_{(0,z,0,0)}(0, 0, 1, 1) &= b_5(1, 0, 0, 0) + b_7(0, 0, 1, 1)
 \end{aligned}$$

The needed calculations yield

$$\begin{aligned}
 (DF)_{(0,z,0,0)}(1, 0, 0, 0) &= F_{z_1} + F_{\overline{z_1}} \\
 (DF)_{(0,z,0,0)}(0, 0, 1, 1) &= F_{w_1} + F_{\overline{w_1}} + F_{w_2} + F_{\overline{w_2}}
 \end{aligned}$$

A further calculation yields

$$\begin{aligned} b_4 &= f_{z_1}^1 + f_{\bar{z}_1}^1 \\ b_6 &= g_{z_1}^1 + g_{\bar{z}_1}^1 \\ b_5 &= f_{w_1}^1 + f_{w_2}^1 + f_{w_1}^1 + f_{w_2}^2 \\ b_7 &= g_{w_1}^1 + g_{w_2}^1 + g_{w_1}^1 + g_{w_2}^1 \end{aligned}$$

Since

$$f_{\bar{z}_1}^1 = 0, \quad g_{\bar{z}_1}^1 = 0, \quad f_{w_1}^1 = 0, \quad f_{w_2}^1 = 0,$$

at a point $(0, z, 0, 0)$ we have

$$A_{\text{Str}} \equiv \begin{pmatrix} b_4 & b_5 \\ b_6 & b_7 \end{pmatrix} = \begin{pmatrix} f_{z_1}^1 & f_{w_1}^1 + f_{w_2}^1 \\ g_{z_1}^1 & g_{w_1}^1 + g_{w_2}^1 \end{pmatrix}$$

Using the truncation of the $D_4 \times \mathbf{T}^2$ -equivariant vector field F given by (3.1), the eigenvalues of $(DF)_{(0,z,0,0)}$, which are not forced to be zero by symmetry, are:

$$\begin{aligned} b_1 &= -\lambda + \mu + 3B_1z^2 + \dots \\ b_3 &= \lambda + \mu + (B_2 - E_2)z^2 + \dots \quad [\text{twice}] \\ A_{\text{Str}} &= \begin{pmatrix} -\lambda + \mu + C_1z^2 + \dots & 2A_1z + \dots \\ A_2z + \dots & \lambda + \mu + \gamma z^2 + \dots \end{pmatrix} \quad [\text{twice}] \end{aligned} \tag{A8}$$

Hence,

$$\begin{aligned} \text{tr}(A_{\text{Str}}) &= 2\mu + (C_1 + \gamma)z + \dots \\ \det(A_{\text{Str}}) &= -2A_1A_2z^2 + \dots \end{aligned} \tag{A9}$$

Note that generically there are no steady state bifurcations in V_4^2 , since generically we can assume that $A_1A_2 \neq 0$. Then the matrix A_{Str} is invertible and has no zero eigenvalues in a neighborhood of the origin. However, Hopf bifurcation can occur in V_4^2 if $A_1A_2 < 0$, since then the matrix A_{Str} can have purely imaginary eigenvalues. This happens when $\text{tr}(A_{\text{Str}}) = 0$.

Recall that stripes $(2, 0)$ solutions satisfy $\mu = \lambda - B_1z^2 + \dots$. On substituting this equation into (A8) and (A9), we obtain the eigenvalues listed in Table 8 for the isotropy subgroup $R_{2,0}$.

Eigenvalues of DF along squares $(2, 0)$ (Tables 11 and 12)

Recall that $S_{2,0}$ solutions have the form (z, z, w, w) with $z, w \in \mathbf{R}$.

Using the truncation up to third-order of the restriction of F to $\text{Fix}((\xi^2)) = \mathbf{R}^4$ given by (5.7), the Jacobian along (z, z, w, w) with $z, w \in \mathbf{R}$ is

$$\begin{pmatrix} A & B & C & C \\ B & A & C & C \\ D & D & E & F \\ D & D & F & E \end{pmatrix}, \tag{A10}$$

where

$$\begin{aligned}
 A &= \mu - \lambda + (3B_1 + C_1 + \beta)z^2 + \beta w^2 + \dots \\
 B &= 2(A_1 w + C_1 z^2) + \dots \\
 C &= z(A_1 + \beta w) + \dots \\
 D &= z(A_2 + 2\gamma w) + \dots \\
 E &= \mu + \lambda + 2B_2 z^2 + (3C_2 + D_2)w^2 + \dots \\
 F &= 2(E_2 z^2 + D_2 w^2) + \dots,
 \end{aligned}$$

and z and w are given by relations (5.2). A further calculation shows that with respect to the basis

$$\{(1, -1, 0, 0)^t, (1, 1, 0, 0)^t, (0, 0, 1, 1)^t, (0, 0, 1, -1)^t\},$$

the Jacobian matrix given by (B.5) becomes

$$\begin{pmatrix}
 A - B & 0 & 0 & 0 \\
 0 & A + B & 2C & 0 \\
 0 & 2D & E + F & 0 \\
 0 & 0 & 0 & E - F
 \end{pmatrix}. \tag{A11}$$

A further calculation shows that the eigenvalues of matrix (A11) are

$$\begin{aligned}
 A - B &= \mu - \lambda - 2A_1 w + (3B_1 - C_1)z^2 + \beta w^2 + \dots = 2(\mu - \lambda) + \dots \\
 E - F &= \mu + \lambda + 2(B_2 - E_2)z^2 + (3C_2 - D_2)w^2 + \dots,
 \end{aligned} \tag{A12}$$

plus the eigenvalues of the 2×2 matrix

$$A_{20} = \begin{pmatrix} A + B & 2C \\ 2D & E + F \end{pmatrix}. \tag{A13}$$

Hence,

$$\begin{aligned}
 \text{tr}(A_{20}) &= A + B + E + F \\
 \det(A_{20}) &= (A + B)(E + F) - 4CD.
 \end{aligned} \tag{A14}$$

Also, notice that $(1, -1, 0, 0)^t$ is the eigenvector corresponding to the eigenvalue $A - B$ and $(0, 0, 1, -1)^t$ is the eigenvector corresponding to the eigenvalue $E - F$.

Taking into account the expressions for $S_{2,0}$ solutions given by (5.2), we notice that in order to determine the stability of $S_{2,0}$ solutions, it is enough to consider linear terms in λ and μ for the eigenvalue $A - B$ (i.e. $A - B = 2(\mu - \lambda) + \dots$), but we need to consider the second-order terms in λ and μ for the eigenvalue $E - F$.

Again, the expressions for S_{20} solutions given by (5.2) allow us to rewrite (A14) as follows:

$$\begin{aligned}
 \text{tr}(A_{20}) &= 2\mu + 2A_1 w + (3\alpha + 2\beta + 2\gamma)z^2 + (\beta + 3\delta)w^2 + \dots = \mu + \lambda + \dots \\
 \det(A_{20}) &= -4A_1 A_2 z^2 + \dots.
 \end{aligned} \tag{A15}$$

Hence, we get the eigenvalues listed in Tables 11 and 12 for the isotropy subgroup $S_{2,0}$.

Note that generically there are no steady state bifurcations due to matrix A_{20} , since generically we can assume that $A_1A_2 \neq 0$. Then the matrix A_{20} is invertible and has no zero eigenvalues in a neighbourhood of the origin. However, Hopf bifurcation can occur in if $A_1A_2 < 0$, since then the matrix A_{20} can have purely imaginary eigenvalues. This happens when $\text{tr}(A_{20}) = 0$.

Eigenvalues of DF along wavy rolls

Recall that wavy-rolls solutions have the form $(0, z, w, -w)$ with $z, w \in \mathbf{R}$ (Table 13).

Using the truncation up to third-order of the restriction of F to $\text{Fix}(\langle \xi^2 \rangle) = \mathbf{R}^4$ given by (5.7), the Jacobian along $(0, z, w, -w)$ with $z, w \in \mathbf{R}$

$$\begin{pmatrix} U_1 & 0 & V & V \\ 0 & U_2 & V & V \\ Z_1 & Z_2 & W & R \\ Z_1 & Z_2 & R & W \end{pmatrix}, \tag{A16}$$

where

$$\begin{aligned} R &= (E_2z^2 - 2D_2w^2) + \dots \\ U_1 &= \mu - \lambda + C_1z^2 + (2D_1 - E_1)w^2 + \dots \\ U_2 &= \mu - \lambda + 3B_1z^2 + (2D_1 - E_1)w^2 + \dots \\ V &= A_1z + \dots \\ W &= \mu + \lambda + B_2z^2 + (3C_2 + D_2)w^2 + \dots \\ Z_1 &= A_2z + \dots \\ Z_2 &= 2(B_2 + E_2)zw + \dots, \end{aligned}$$

and z and w are given by relations (5.8). A further calculation shows that with respect to the basis

$$\{(1, 0, 0, 0)^t, (0, 1, 0, 0)^t, (0, 0, 1, 1)^t, (0, 0, 1, -1)^t\}$$

the matrix given by (A16) becomes

$$\begin{pmatrix} U_1 & 0 & Z_1 & 0 \\ 0 & U_2 & Z_2 & 0 \\ 2V & 2V & W + R & 0 \\ 0 & 0 & 0 & W - R \end{pmatrix},$$

and its eigenvalues are $W - R$, corresponding to the eigenvector $(0, 0, 1, -1)^t$ and the eigenvalues of the 3×3 matrix

$$A_{WR} = \begin{pmatrix} U_1 & 0 & Z_1 \\ 0 & U_2 & Z_2 \\ 2V & 2V & W + R \end{pmatrix}.$$

Substituting z and w given by (5.8) into $W - R$ and into matrix A_{WR} , we get:

$$W - R = 4\delta w^2 + \dots \tag{A17}$$

and

$$A_{WR} = \begin{pmatrix} U_1 & 0 & Z_1 \\ 0 & U_2 & Z_2 \\ 2V & 2V & Q \end{pmatrix}, \tag{A18}$$

with

$$\begin{aligned} Q &= 2(E_2z^2 + 2C_2w^2) + \dots \\ U_1 &= 2B_1z^2 + \dots \\ U_2 &= (C_1 - B_1)z^2 + \dots \\ Z_1 &= A_2z + \dots \\ Z_2 &= 2(B_2 + E_2)zw + \dots \\ V &= A_1z + \dots, \end{aligned} \tag{A19}$$

that is, we obtain the eigenvalues listed in Table 13 for the *wavy rolls* solutions.

Eigenvalues along stripes (2, 2)

Recall that $R_{2,2}$ solutions have the form $(0, 0, 0, w)$ with $w \in \mathbf{R}$ (Table 12).

Using the truncation up to third-order of the restriction of F to $\text{Fix}(\langle \xi^2 \rangle) = \mathbf{R}^4$ given by (5.7), the Jacobian along $(0, 0, 0, w)$ with $w \in \mathbf{R}$ is

$$\begin{pmatrix} \mu - \lambda + D_1w^2 + \dots & A_1w + \dots & 0 & 0 \\ A_1w + \dots & \mu - \lambda + D_1w^2 + \dots & 0 & 0 \\ 0 & 0 & \mu + \lambda + D_2w^2 + \dots & 0 \\ 0 & 0 & 0 & \mu + \lambda + 3C_2w^2 + \dots \end{pmatrix},$$

where $\mu = -\lambda C_2w^2 + \dots$. It is easy to get the eigenvalues listed in Table 12 for the isotropy subgroup $R_{2,2}$.

Copyright of *Dynamical Systems: An International Journal* is the property of Taylor & Francis Ltd and its content may not be copied or emailed to multiple sites or posted to a listserv without the copyright holder's express written permission. However, users may print, download, or email articles for individual use.